Development of Auditory Brainstem Response in the Big Brown Bat

DEVELOPMENT OF AUDITORY BRAINSTEM RESPONSE IN THE BIG BROWN BAT

By THOMAS C. G. GROULX, B.Sc.

A Thesis Submitted to the School of Graduate Studies in Partial Fulfilment of the Requirements for the Degree Master of Science

Lay Abstract

The development of hearing within the big brown bat was measured from birth to maturation. Hearing development was measured using the auditory brainstem response (ABR), a multi-featural signal which is widely accepted as a measure of auditory functioning. Two observers found closely matching labels relating to ABR presence/absence and these labels related well to ABR features of interest including root mean square signal amplitude, spectral composition of the evoked signal, as well as relationships to ABRs evoked at other frequencies and amplitudes. The ABR features of interest showed greater sensitivity to stimulus level outside of the acoustic fovea of the bat, which shifted upward in frequency as bat pups matured.

Abstract

Echolocating bats use hearing for passive orientation, alerting functions, and social communication. How bats develop their sense of hearing is an important question that can help us understand hearing in all mammals, including humans. This knowledge is also useful to outline the typical hearing of different animal models to provide information for modeling hearing development. Here, I document the neural progression of hearing in developing pups of the big brown bat, *Eptesicus fuscus.* Hearing development was tracked by measuring the auditory brainstem response (ABR) at multiple timepoints during pup maturation and evaluating changes in the recorded neural waveforms. Audiograms were measured as the ABR threshold at different sound frequencies. The ABR waveform consists of several peaks and troughs that represent the synchronous and summed responses of ascending auditory neurons between the cochlea and the upper brainstem. To a trained observer, signatures of ABR peaks and troughs indicate whether a stimulus has evoked a reliable neural response. The threshold of audibility was determined by repeatedly presenting pure tone stimuli, starting at a high sound pressure level (SPL) and systematically reducing stimulus level until the recording no longer showed a time-locked response. An advantage of using ABRs is the procedure is a relatively non-invasive, hence it allows for multiple, longitudinal recordings from the same individuals across development. I analyzed a series of ABR recordings looking for changes in waveforms features related to the onset and maturation of hearing in *E. fuscus* pups. First, I measured changes in the average root mean square amplitude of

ABR signals as pups aged. A spectral analysis of ABR waveforms was conducted, focusing on 2 frequency regions of interest. A cross-correlation analysis was used to measure changes in neural response latency as stimulus SPL was varied but also to measure the time-lag evoked by the same stimuli in pups at different ages. My results demonstrate that amplitudes in ABRs increased with pup age and stimulus SPL, and that this effect was frequency dependent, decreasing as the stimulating tone was moved away from frequencies close to the bat's auditory fovea (i.e. the frequency range of best auditory sensitivity between 20 and 48 kHz). Changes in stimulus SPL affected the latency of ABR signals, although the effect was less pronounced for tones within the bat's auditory fovea. My research describes the development of the auditory system of the big brown bat as measured by ABRs. The development of bat tuning curves as described by ABRs are compared to those described by behavioural data.

Acknowledgements

Thank you to Dr. Paul Faure for your guidance and for always encouraging me to pursue new and interesting questions. Many thanks to Dr. Doreen Möckel for collecting the ABR neural recordings from bat pups and for her emotional support and scientific expertise. Thanks to all my friends, colleagues, and family for always encouraging me to reach my goals, pushing me to be a better scientist, and for putting up with me. Thank you to the animal care staff who cared for our animals with unrivaled passion. Thank you to my wife, for her patience, love, and understanding. Lastly, thank you to all the bats that gave their lives for science.

List of Figures

Figure 1. Example averaged ABR waveform ‘stack’, collected at decreasing stimulus amplitudes from a single PND 90 pup at two stimulus frequencies: 20 kHz (*top*) and 48 kHz (*bottom*)..... 44

Figure 2. Tuning curve (audiogram) of young adult bat at post-natal day (PND) 60. 46

Figure 3. Variation in the temporal position of ABR peaks recorded in developing bat pups..... 48

Figure 4. Comparison of independent determination of ABR thresholds as judged by two observers. 50

Figure 5. Root mean square (RMS) energy (μV) of recorded ABR signal as a function of stimulus level re threshold, uncorrected for all ages of animal and frequency of stimulating tone..... 51

Figure 6. Example ABR waveform stack with its associated cross-correlation function stack..... 52

Figure 7. First order linear regression of the peak correlation cross-product value for a given ABRs as a function of the highest stimulus level (re threshold) in its stack. 53

Figure 8. Second (A) and third (B) order regressions of frequency and cross-correlation product..... 54

Figure 9. Average fast Fourier transform (FFT) of ABR waveforms evoked from each stimulus frequency..... 56

Figure 10. .. Regression analysis of peak cross-correlation product shift modelled as a function of stimulus level re threshold. 57
Figure 11. Regression analysis of FFT integrals for two spectral ranges in ABR waveforms. 58
Figure 12. Linear and quadratic regressions of rms using age as a regressor. .. 59
Figure 13. Root mean square (µV) signal energy as a function of stimulus frequency (Hz) for increasing age categories in big brown bat pups. 60

Declaration of Academic Achievement

I, Thomas C. G. Groulx, do solemnly swear my allegiance to the scientific method as a proper way of knowing and I have authored the work in this thesis.

Table of Contents

Lay Abstract iii

Abstract iv

Acknowledgements vi

List of Figures vii

Declaration of Academic Achievement ix

Table of Contents x

Introduction 1

Materials and Methods 9

- Animals 9
- ABR electrophysiology 10
- Acoustic chamber 11
- Acoustic stimuli 12
- ABR threshold estimation 13
- Data analysis 15

Results 18

- ABR threshold analysis 18
- RMS amplitude analysis 19
- Cross-correlation latency analysis 21
- FFT spectral power analysis 24

Discussion 26

References 35

Appendix—Figures 44

Introduction

It is difficult to find an animal that relies on auditory processing more than the echolocating bat. Accordingly, bats have evolved an impressive set of auditory processing skills that have benefited them. Bats tend to have high sensitivity to sounds containing energy at frequencies near their range of vocalizations (Jen, Zhou, & Wu, 2001; Ehrlich, Casseday, & Covey, 1997), extremely accurate frequency resolution (Koay, Heffner, & Heffner, 1997), precise temporal resolution (Pinheiro, Wu, & Jen,1991), robust sound localization (Brewton, Gutierrez, & Razak, 2018) and an excellent ability to extract useful information from signals in noise (Møhl & Surlykke, 1989). While much is known about bat hearing and the underlying auditory processing mechanisms, less is known about how these abilities develop from birth. The auditory system of the developing bat moves from a state of near deafness to the stellar auditory processing abilities of the adult in a relatively short time period. Observing how the bat's auditory system changes over this short time frame provides an excellent opportunity to study early mammalian auditory development.

There is evidence that the auditory processing abilities of bats are achieved, at least in part, through nurtured developmental processes. Most bats do not show behavioural evidence of hearing until after their first week of life—an example of which is found in the baby pallid bat who will begin to respond to their mother's directive calls by decreasing the period (i.e. increasing the repetition rate) between emitted isolation calls (Brown, Grinnell, & Harrison, 1978). Like many other mammals, there is also neurological evidence that auditory

experience during development affects the emerging bat auditory system (Kral, Tillein, Heid, Harmann, & Klinke, 2004). For example, in the moustached bat, it has been found that newborn sound exposure relates to both neuron sensory field attributes in the auditory cortex as well as the overall rate of change of cortical organization (Froemke & Jones, 2011).

Like the moustached bat and many other bat species, audiograms generated using data from cochlear microphonics to different frequency stimuli of adult big brown bats (*Eptesicus fuscus*) demonstrate a high sensitivity for sounds containing frequencies found in their echolocation calls (Dalland, Vernon, & Peterson, 1966). The development of this spectral sensitivity appears to originate, in part, from the selective gain provided by the bat's pinnae, whose outer ear structures have been implicated in the development of some frequency-specific cancellation between two threshold minima in the behavioural audiogram (Koay et al., 1997; Macias, Mora, Coro, & Kössl, 2006). While part of this variation in frequency sensitivity relates to outer ear structures and cochlear specializations, adult bats have higher-order auditory processing centers along the central auditory pathway that maintain this frequency specialization; they also have a greater representation for higher frequencies relative to lower frequencies (Casseday & Covey, 1992). There are some indications that bats are not born with this frequency specialization, but rather it is the product of some set of developmental processes that occur largely after birth. Measuring the change in big brown bat auditory functioning as they mature can help provide an understanding of the effects of these developmental processes.

Among other methods, one relatively non-invasive technique to measure change in auditory functioning throughout an animal's development is the auditory brainstem response (ABR). The ABR is an extracellular measure of a neural response to an auditory stimulus. By placing contact or subdermal electrodes near the auditory bullae at the base of the skull and repeatedly presenting a stimulus and averaging the response, the ABR emerges as a short latency, synchronous, time-locked waveform (Shaw 1988). An ABR can be recorded from animals at any age and without prior behaviour training, giving it an advantage over behavioural methods for outlining changes in animal hearing during early development. Signature oscillation peaks of ABR waveforms are typically labelled with roman numerals in the order they appear over time (i.e. peaks I-IV, I-V, I-VI, or I-VII, depending on animal). These peaks reflect the synchronous and summed responses of ascending auditory neurons between the cochlea and upper brainstem (Burkard & Moss, 1994; Melcher & Kiang, 1996). The recording technique makes it difficult to deduce the exact anatomical origins of variations in the signal. It is generally accepted, however, that the peaks roughly represent the sum of synchronous activity in areas neighbouring the electrode. The first peak of an ABR is generally found to represent the activity of the vestibulocochlear nerve. Increasingly latent peaks are found to represent sums of synchronous potentials of increasingly higher (along the central auditory pathway) processing areas, including the cochlear nucleus, superior olive, and inferior colliculus (Boku, Riquimaroux, Simmons, & Simmons, 2015; Benichoux, Ferber, Hunt, Hughes, & Tollin, 2018). In other words, the latency of a given peak

in an ABR waveform increases as sounds are processed by the different nuclei along the central auditory pathway. Variations in the timing and amplitude of these peaks have been shown to relate to variations in the auditory stimulus as well as in the functionality of auditory processing (Di Lorenzo, Foggia, Panza, Calabrese, Motta, Tranchino & Lombardi, 1995; Gorga, Reiland, Beauchaine, Worthington, & Jesteadt, 1987; Don, Kwong, & Tanaka, 2005; Stapells & Oates, 1997; Wrege & Starr, 1981).

As the amplitude of an acoustic stimulus decreases, the peak amplitudes of an associated ABR will also decrease while the waveform latency (particularly of peak V) increases (Stapells & Oates, 1997; Simmons, Moss & Ferragamo, 1990). Lowering the stimulus amplitude will eventually reduce the amplitude of the ABR signal to where it is no longer detectable against the background noise. Determining the lowest amplitude acoustic stimulus that still produces a measurable ABR across an array of frequencies produces a threshold tuning curve for the animal. Likely due to the summed far-field nature of the response, tuning curves derived from ABRs are often less sensitive than those measured from single neurons or behaviorally. This is because summed far-field responses represent the compound response of all neurons in the field, including those related to the evoked excitation as well as unrelated neural responses. Therefore, recordings using the summed-far field method will be likely to have values less extreme than single-unit recordings which collect an individual response relating to activity in a single neuron uninfluenced by external activity. However, where ABRs are less sensitive, they are reliably and equally less

sensitive at most frequencies—meaning that while we may not get the exact threshold from an ABR, a reliable tuning curve can still be produced (Munnerley, Greville, Purdy, & Keith, 1991; Kenyon, Ladich, & Yan, 1998).

A variety of methods exists to produce a tuning curve. Most methods produce a unidimensional result for a given acoustic stimulus (detectable = true/false). An ABR evoked by a given acoustic stimulus has the added benefit of producing an analyzable vector as an output. This vector allows for analyses of whether different auditory signals are measurable by ABRs, as well as simultaneous analysis of the variation between signature oscillations as a representation of variance within the higher-order areas of early central auditory processing.

Commonly analyzed features of ABR signals are the 4-5 most observable waveform peaks. But there are issues with this analysis that largely relate to the variability in labelling different ABR peaks. The presence and location of specific peaks are conventionally labelled visually by experts (Cone-Wesson, Dowell, Tomlin, Rance & Ming, 2002; Don, Elberling & Waring, 1984; Stapells & Oates, 1997). Furthermore, ABR signatures in less-used animal models are less described, and often do not fit ABR conventions. The variation and ambiguity of animal ABR recordings makes the signals difficult to classify and this has likely contributed to the current convention of visual labelling waveform peaks. It has also been shown that different experts have relatively low inter-rater reliability for signals evoked near stimulus threshold (Alpsan & Ozdamar, 1992). In addition to obvious replication issues, this measurement error makes it more difficult to

utilize ABRs in experimental and diagnostic settings. As ABRs are less time-intensive and less invasive than other hearing threshold methods, it is valuable to create objective criteria that can be used in the analysis of ABR signals.

An in-depth analysis of different peaks in ABR waveforms measured throughout a bat's development may help us characterize maturational changes in central auditory processing. Changes in the height, width, and latency of different ABR waveform peaks informs about the strength, synchrony, and timing of the evoked response. Moreover, a small number of different computational approaches have been attempted to create objective descriptions of ABRs in non-human animals (Walsh, McGee & Javel, 1986; Brittan-Powell & Dooling, 2004; Song, McGee & Walsh, 2008). Detecting the presence of an evoked ABR has been achieved by comparing relative signal power in recorded waveforms (Wong & Bickford, 1980; Linnenschmidt & Wiegrebe, 2019). Comparative correlation procedures were found to be comparable to visual assessment in detecting the presence of an ABR when stimuli were well above threshold (Arnold, 1985). More rarely, objective detection of signature oscillations within an ABR has been attempted (Cebulla, Stürzebecher, & Wernecke, 2000; Don et al., 1984). In humans, peak presence has been calculated using zero crossings on the first derivative of the ABR signal, and peak labels were assigned according to the specific time window that a crossing was detected (Gabriel, Durrant, Dickter, & Kephart, 1980). Again, this approach was only used with ABRs evoked by suprathreshold stimuli and the ABR signals were pre-selected to ensure they had all five signature peaks. This analysis was only marginally successful in

achieving peak identification and the success decreased further when analyzing waveforms with lower signal to noise ratios.

Spectral analyses have also been used to detect and label of ABR waveform peaks using a scrolling Fast Fourier transform (FFT) window (Fridman, John, Bergelson, Kaiser, & Baird, 1982). Using variations in frequency improved the detection and identification of ABR peaks, but the method still failed to reach high levels of accuracy where stimulus levels were lowered and near threshold. In this study, I have employed some of these signal classification and analysis techniques on ABR waveforms collected from developing big brown bats to aid in outlining how central auditory processing changes as pups mature and to give guidance on possible analyses methods that could be used for future automated classification of ABRs. Methods designed for this purpose should keep in mind the increased variance between animal models and that best features used in these methods could differ from the specific features used in human models.

The aforementioned experiments and future studies could benefit from an in-depth study of the development of ABR waveform features in non-human animals. The techniques used in this thesis include measuring the root mean square (RMS) amplitude, identifying spectral components, and temporal changes in the ABR signals recorded from developing *Eptesicus fuscus* pups and outline how these features vary with age and the frequency / amplitude of the stimulating tone. I expect amplitude information, found by both a RMS and FFT analysis, to vary with age and stimulus SPL above threshold. Given that ABRs often have some spectral component related to the frequency of the stimuli, a FFT analysis

is expected to show spectral variation between different stimulating frequencies and suprathreshold *versus* subthreshold tones. A previous study used ABRs to measure the development of threshold tuning curves during in *E. fuscus* pups (Möckel, Groulx, & Faure, 2021), however, to the best of my knowledge, a comprehensive study of maturational changes in ABR waveforms has not been previously assessed.

Materials & Methods

Animals

Big brown bat (*Eptesicus fuscus*) pups used in this study were part of a captive breeding colony. Wild bats from southern Ontario were caught and housed in a husbandry facility at McMaster University, Ontario, Canada. Within the facility, bats were freely permitted to fly and interact with other bats. The temperature and lighting of the facility varied with ambient conditions (Skrinyer et al., 2017). Each year, captive mating occurs in the colony, hence pups used in this study were born to either wild-caught bats or to their direct descendants. ABRs were recorded on 22 juvenile bats, for the first time starting between post-natal day (PND) 10 and PND 13 (PND 13 was used instead of PND 10 if both ear canals were not yet open or if other recording issues occurred on PND 10). A subset of pups was rerecorded every 3 days until PND 31, which is approximately when *E. fuscus* begin to successfully echolocate (Mayberry & Faure, 2015; Mayberry, Faure, & Ratcliffe, 2019). A subset of these same 22 animals were tested again at PND 60, PND 90, and 1 year of age (Möckel et al., 2021).

Pregnant females near parturition were either isolated or held in small groups and housed in stainless steel wire mesh holding cages (28 x 22 x 18 cm; l x w; h) for closer monitoring of pup birth dates. The day of birth was designated as postnatal day (PND) 0. From PND 0 to PND 31, recorded bats were housed with their mother and any siblings. Mother bats and weaned pups were given *ad libitum* access to food (mealworms; Reptile Feeders, Norwood, ON) and water.

When pups were one month old (PND 31), they and their mothers were housed in the captive colony.

ABR electrophysiology

Before recording, pups were given a subcutaneous injection of an anaesthetic [4:1 v/v mixture of 1 mg/mL midazolam plus 50 µg/mL fentanyl citrate; Sandoz Canada Inc., Boucherville, Quebec]. The injection volume was adjusted according to the mass, activity, and drug experience of the pup (for details, see Möckel et al., 2021). Five pups that were calm enough during their first two recordings (PND 10 and 13) did not require anaesthesia. Pups that became active during testing were removed from the recording chamber and given a top-up dose of anaesthetic, as needed. Animals who became too active to complete a full recording were retested the following day and if this recording was successful, the data were pooled with the data collected from the previous attempt (if any).

Following injection, the feet and torso of anesthetized pups were wrapped in panty hose leaving the head exposed. Recording was enabled by placing three needle-electrodes (3-lead disposable, 27-gauge, 13 mm, Rochester Electro-Medical, Lutz, Florida, USA) inserted subcutaneously on the pup's head. One differential lead was placed behind the ipsilateral ear, a second differential lead was placed at the base of the skull, and the ground lead was placed behind the contralateral ear. Signals were amplified 20x by a low impedance head stage from Tucker Davis Technologies (TDT RA4LI), whose output was further amplified 250x and digitized by a preamplifier (TDT RA4PA Medusa, sampling

rate 25 kHz) before passing the signal to a multifunction processor (TDT RX6) via a fiber optic cable. At the end of each recording session, electrodes were manually removed and cleaned with 95% ethanol. Full details of the ABR recording equipment and experimental procedures are given in Möckel, et al., (2021).

Acoustic chamber

Wrapped pups were placed on a foam pad atop a raised (10 cm) plexiglass platform (13 x 15 x 0.3 cm) inside an angle-iron Faraday cage (50 x 40 x 60 cm). The top and walls of the cage were lined with grounded copper mesh and sound-attenuating foam (Sonex® Classic; Pinta Acoustic, U.S.A.), except for one side facing the experimenter which could be temporarily covered by a removeable foam panel. Recordings took place at laboratory room temperature and humidity.

The loudspeaker was placed in the corner towards the right of the opening in the cage, 10 cm from the platform and facing towards the platform. Following anaesthetic injection, bats were wrapped in nylon cloth before being placed on a foam pad, oriented in a manner which allowed the bat's right ear canal to be pointed toward the loudspeaker before the electrodes were placed. The recording electrode was placed near and alongside the protrusion of the pup's right outer ear (which is pointed at the speaker). The reference electrode was placed in the same position alongside the contralateral ear with the ground wire placed in-between the recording and reference electrode. One the bat was situated, the foam panel was placed to cover the hole-side of the cage, at this point stimuli production and response recording could begin.

Acoustic stimuli

Sound stimuli were created and played using BioSigRP commercial software (Tucker-Davis Technologies). Sounds were digitally generated with a multifunction digital signal processor (TDT RX6; 260 kHz sampling rate) connected to a programmable attenuator (TDT PA5), broadband electrostatic driver (TDT ED1) and free-field electrostatic loudspeaker (TDT ES1, frequency response flat ±11 dB from 4-110 kHz). The loudspeaker was positioned slightly below the bat's auditory horizon approximately 45° off the animal's midline and at a distance of 10 cm from the right ear. All recordings were collected with the right ear ipsilateral to the loudspeaker.

The loudspeaker was calibrated with a ¼-inch condenser microphone (0° incidence, grid off; B&K Type 4939, Naerum, Denmark) placed 10 cm in front of the loudspeaker. The microphone output was connected to a measuring amplifier (B&K Type 2610) whose AC output was fed to a stereo microphone amplifier (TDT MA3) connected to the RX6 processor. The output of the loudspeaker was reference to a sound calibrator (B&K type 4231) and expressed in decibels sound pressure level (dB SPL re 20 µPa) equivalent to the peak amplitude of continuous tones of the same carrier frequency. Broadcast tones at all frequencies were compensated in software and equalized in magnitude to a maximum output of 85 dB SPL. All tones had 2.0 ms rise/fall times shaped with a squared cosine function.

Stimulus tones lasted 5 ms in duration and were followed by 5 ms of silence, allowing for a 10 ms recording window. The recording window was

followed by an additional 37.62 ms of silence (not recorded), yielding an interstimulus interval = 47.62 ms. Tones were repeated 512 times at each frequency-level combination at a presentation rate of 21 Hz. A running average of the recorded ABR was digitally bandpass filtered (low-pass cutoff frequency = 3 kHz, high-pass cutoff frequency = 10 Hz, notch frequency = 50 Hz) and stored on computer. Recorded ABRs were further high pass filtered (high-pass cutoff frequency = 150 Hz) before they were exported for visualization and analysis.

Each pup was presented with pure tones at 10 stimulus frequencies (4, 8, 10, 16, 20, 32, 48, 64, 80, and 100 kHz) and at amplitudes ranging from 5 to 85 dB SPL (for each session, tones was presented in the above order). If an ABR was note successfully recorded at each frequency (usually because the pup was active and moving during a session), the data were discarded, and the animal was retested the following day.

ABR threshold estimation

During a recording session, the first stimulus of each frequency was presented at 75 dB SPL. If an ABR was visually detected, then the signal amplitude was decreased until a time-locked response was no longer visible. If an ABR was not visually detected at 75 dB SPL, the signal amplitude was increased until an ABR signal was visually detected or until reaching the maximum system amplitude of 85 dB SPL. In searching for an animal's threshold at a given frequency, changes to stimulus amplitude were informed by the perceived strength of the evoked ABR. If the amplitude of the evoked ABR seemed large and prominent, large decreases in SPL (in 10- to 20-dB steps) were made to the stimulus. When the

amplitude of the evoked response became smaller and more difficult to detect, smaller changes in stimulus SPL (3- to 5-dB steps) were made until an ABR was no longer visible against the background noise. We then increased the amplitude of the stimulus in 1- to 3-dB steps until an ABR waveform was again visible and deemed that SPL as the acoustic threshold (see Fig. 1). This procedure was repeated, in order, for the remaining higher stimulus frequencies to create an ABR threshold tuning curve. Because the maximum output of our stimulus delivery system was 85 dB SPL, in some bats (e.g. young pups tested at high ultrasonic frequencies) auditory thresholds at some frequencies could not be determined.

We then increased the stimulus SPL in 1- to 3-dB steps until an ABR waveform was again visible and deemed that SPL as the acoustic threshold (e.g. arrows in Fig. 1). We repeated this procedure, in order, for the remaining higher stimulus frequencies to create a tonal ABR threshold tuning curve. Because the maximum output of our stimulus delivery system was 85 dB SPL, in some animals (e.g. young pups tested at high ultrasonic frequencies) auditory thresholds at some frequencies could not be determined.

Threshold estimates were judged by two, independent observers. The first observer (Doreen Möckel) collected the recordings and determined thresholds online with the aid of a stacked plot display (Fig. 2). The second observer (Thomas Groulx), blind to the threshold estimates of the first observer, re-estimated thresholds from the same recordings also using a stacked plot display. The stacked plot display allowed both observers to visually scan the amplitude

and latency of the evoked response across all waveforms collected from a bat and integrate this information to inform threshold judgements.

Data analyses

The ABR waveform features I investigated included the root mean square (RMS) amplitude, latency, spectral distribution of energy and the relationship of these variables to stimulus amplitude, stimulus frequency, animal ID, and age. Each feature below was measured from the 1 to 8 ms segment of the 10-ms ABR recording window.

i. Root Mean Square (RMS) Amplitude Analysis

I calculated the RMS amplitude of an ABR waveform with the following equation:

$$RMS = \sqrt{\sum_{i=0}^{n} \frac{x_i^2}{n}},$$

where x_i is the amplitude value at a given time point. I used ordinary least squares regressions to determine the relation between stimulus frequency and RMS amplitude and how this relationship varied with animal age. I also compared the RMS values for ABR signals visually labelled as above and below threshold. Both first and second order linear regressions were performed to compare relative fit. The regressions used both raw calculated RMS as well as RMS corrected for variation due to age, animal, and frequency.

ii. Latency Analysis

Conventional detection and peak labeling proved unreliable for the ABRs of younger bats and the presence of distinct peaks were difficult to algorithmically

detect using simple linear models. Therefore, a cross correlation analysis was used to obtain a measure of ABR waveform latency as a function of stimulus amplitude and frequency, and pup age. Because ABRs evoked at the highest SPLs had the most prominent peaks, I used a cross-correlational analysis to compare the relative ABR latency evoked by lower amplitude tones and assessed latency changes across stimulus frequency and bat age. Welch's t-test was used to compare differences between recordings visually-labelled as containing an ABR *versus* those not containing an ABR and used least squares regression for analyzing trends within suprathreshold responses.

iii. Spectral Power Analysis

A Fast Fourier Transform (FFT) analysis was performed on all recorded signals—both on responses visually-labelled as containing an ABR (for stimulus amplitudes of >5 dB above threshold) and those labelled as not containing an ABR—and measured and compared the difference in power using Welch's t-test. Two sections of the magnitude spectrum of each ABR were analyzed: 0-1000 Hz and 1000-2000 Hz. A power analysis was performed using Cohen's D. The FFTs were calculated with a Hanning window and were zero-padded using the Scipy Python Package (Virtanen et al., 2020). The relationships to age, stimulus frequency, and SPL were analyzed using least squares regression.

Unless otherwise stated, analyses were performed on ABR signals visually labelled by experimenters as being above threshold. For all regression analyses, I used least squares regression with correlation coefficients (R) and/or coefficients of determination (R^2) to obtain best-fit linear models of the

progressive change in auditory sensitivity with age at each frequency, and multiple linear regressions with Bonferroni corrections to test for slope differences between frequencies. Age spanned between PND 13 and PND 95 (newborn to adult), and stimulus amplitudes spanned between 0 and +66 dB re threshold.

Results

ABR threshold analysis

Plotting the hearing threshold at each tested frequency yields an audiogram that can be compared across animal ages (Fig. 2). Additional examples of how the audiogram of *E. fuscus* changes in pups as they age were recently published (Möckel et al., 2021). The ease with which ABRs could be visually labelled varied widely depending on the frequency of the stimulus and age of the animal tested. Some ABR waveform stacks had common signatures between recordings which were easily detectable while others were noisy and difficult to detect (e.g. Fig. 1). The typical set of peaks 1_V in ABR waveforms collected from developing pups were difficult to visually detect. The average position (ms) of the largest amplitude waveform peak, as determined by the location of the peak with the greatest height among the 5 most prominent peaks of a waveform, within a stack (unique animal, frequency, age combination) varied by more than half (50%) of the 10-ms recording window (Fig. 3), with the number of peaks also varying widely (data not shown). Such variation made it difficult to perform a simple peak analysis on pup ABRs as a function of animal age and for changes in stimulus frequency or level.

Given the difficulty required to label, it was important to verify the original threshold estimates before further determining how features of bat ABR waveforms vary with pup age and stimulus parameters. I conducted a blind analysis and re-estimated ABR thresholds from a subset of animals using the raw waveforms that the first observer used to estimate hearing thresholds during

electrophysiological recording. Figure 4a plots the threshold difference between the two observers for seven *E. fuscus* pups. Positive values indicate the blind observer judged thresholds to be higher (less sensitive) than those measured during recording. Note the cluster of points near 0 dB, which indicates that both observers were fairly consistent in their threshold estimates using the raw waveforms. The mean ± SD threshold difference between the two observers for the seven pups was 2.9 $\pm$ 7.15 dB (n = 289 observations). The distribution of absolute values of threshold differences revealed that 73.7% of observations were within 5 dB and 86.9% were within 10 dB between the two observers (Fig. 4b). Owing to the high interobserver reliability (r^2 = 0.88327, p<<0.0001), the remaining analysis in this thesis uses thresholds estimated by the first observer.

RMS amplitude analysis

Based on a previous study that examined the power in ABR waveforms from developing bat pups (Linnenschmidt & Wiegrebe 2019), I predicted that a regression analysis on the root mean square (RMS) amplitude of recorded signals would increase as stimulus level was increased. An ordinary least squares regression analysis showed that stimulus level re threshold accounted for a small but significant sum of the variation in the RMS amplitude of ABR waveforms (R^2 = 0.199, intercept = 116.8637 µV + 2.48 µV/dB; p = 3.305e-135) (Fig. 5a). When analyzing this relationship within an ABR waveform stack (where adjustments were made to the models to account for age, animal ID, and stimulus frequency), the model were able to explain notably more variance (R^2 = 0.257; p = 1.215e-180; Fig. 5b). Including age as a variable resulted in a notable

increase in the variance accounted for by the model (R^2 = 0.213 and R^2 = 0.271 for unadjusted and adjusted models, respectively) showing a significant sum of variation accounted for by age ($p \leq 2.613e-012$) and a positive relationship between age and RMS. As animals aged, the RMS amplitude of the ABR signal tended to increase (~0.586 µV/day on average across all frequencies).

Frequency had an unexpected interaction with age, where the effect of frequency alone was nonsignificant in accounting for variation in the RMS amplitude of ABR signals even prior to Bonferroni corrections. There was, however, a frequency-dependent effect of age on RMS amplitude. This relationship demonstrated a significant increase ($p << 0.00005$) in RMS amplitude per day for ABRs collected with middle hearing range tones (i.e. 20, 32, and 48 kHz) relative to lower (4, 8, 10, and 16 kHz) or higher frequency tones (64, 80, and 100 kHz) with RMS increases over age in higher frequency tones being greater ($p << 4.8e-4$) than that of lower frequency tones. In other words, ABR waveforms recorded in response to tones of higher frequencies tended to see greater increases in RMS amplitude over development.

The frequency of stimulating tone also had an interaction with stimulus amplitude re threshold in predicting changes in the RMS amplitude of ABR signals, where changes to the stimulus level re threshold of frequencies in the lowest (4, 8, 10, and 16 kHz) and highest signals presented (64, 80, and 100 kHz) had a smaller effect ($p << 0.00005$) on the RMS amplitude of recorded ABRs (mean change in RMS amplitude= 0.861/dB re threshold) relative to the increases observed (mean change in RMS amplitude = 3.138/dB re threshold) for

stimulus frequencies in the middle range (i.e. acoustic sweet spot; 20, 32, and 48 kHz) of bat hearing. Modelling dB re threshold, frequency, age, and their interactions accounted for a notable sum of the overall variance in the RMS amplitude of recorded ABR waveforms (R^2 = 0.391, p = 4.33e-273).

Cross-correlation latency analysis

Owing to the difficulty in visually identifying distinct ABR peaks, changes in ABR waveform latency with changes in stimulus level re threshold were often difficult to describe. Peaks in the recorded ABRs of developing pups were small, varied in number, and had irregular relationships with respect to peaks of other ABRs in the same waveform stack (e.g. see Fig. 1b). This ABR variability rendered static methods of automated peak detection ineffective. Hence, I used a cross-correlation analysis to describe changes in the evoked ABR latency without using waveform peak features. During ABR visual labelling, one strategy for expert labellers has been described as a 'mental cross-correlation' (Delgado & Ozdamar, 1994) where higher dB signals within a stack (same animal, frequency, day ABR recordings) are mentally cross-correlated with responses evoked by lower amplitude stimuli. If the peak value of the cross-correlation is too low or if the lag of the cross-correlation falls outside of the theoretical expected temporal value, a recording would be deemed to not contain an ABR. I calculated cross-correlations functions within a stack of ABR waveforms by cross-correlating the ABR evoked by the highest amplitude stimulus to each ABR evoked by successfully lower amplitude stimulus tones and measured the cross-correlation

peak and lag time values as a function of stimulus amplitude re threshold while noting any potential interactions with animal age or stimulus frequency.

Cross-correlation calculations provide the maximum possible overlap between recorded signals, in addition to the relative time-shift (lag) of those signals to achieve maximum correlation. This allowed me to obtain a measure of shift per dB of inducing tone for different stimulus amplitude despite being unable to reliably and routinely identify key ABR peaks. This method would be expected to result in higher-error relationships between dB of inducing tone and lag of cross-correlation than lag calculations that employ waveform peak identification as it included a greater ratio of noise: signal of the ABR than would be presumed using peak calculations. Many bat ABRs tended to vary significantly (Fig. 2) and therefore peak correlations were expected to be relatively weak. Given the positive correlation between ABR RMS amplitude and stimulus level re threshold, peak evoked responses were assumed to be most reliable in ABRs induced by the highest amplitude stimulating tones, thus cross-correlations functions were calculated between any given ABR in a stack and the ABR evoked by the highest stimulus amplitude for the same frequency/animal/age combination. “Cross-correlation output” refers to the output of a cross-correlation function between an ABR induced by a given dB SPL tone on a particular frequency/day/animal combination and the ABR induced by the highest dB SPL tone for that combination (e.g. Fig. 6). As such, ABRs evoked at the highest SPL within a stack do not have an associated cross-correlation measure for further analysis because the peak value of auto-correlation is always 1.0 at a time lag of zero.

First, comparisons of peak cross-correlation values were made between waveforms labelled as containing an evoked ABR and those not containing an ABR. I predicted that neural recordings pre-labelled as containing an evoked ABR were expected to have higher peak cross-correlation values than recordings without an ABR, and the difference in peak correlation value was significant between recordings labelled as containing or not containing an evoked ABR (Welch's t-test p = 3.4808e-10, Cohen's D = 0.14).

I used least squares regression to determine the degree to which changes in stimulus level re threshold accounted for variation in peak cross-correlation product values. There was a weak positive significant relationship between stimulus level re threshold and the peak cross-correlation value (R^2 = 0.214, p = 1.43506e-25). When combined with age, the models could account for slightly more variation, showing a significant interaction between age and SPL re threshold, where the cross-correlation product of younger animals was more sensitive to changes in stimulus level compared to older animals (Fig. 7). Using solely age to model peak cross-correlation product accounted for even less variance ($R^2 \leq 0.005$). Modelling peak cross-correlation product using frequency could account for a small sum of the total variation (R^2 = 0.015), accounting for slightly more variation when second order (R^2 = 0.0394) and third order (R^2 = 0.0616) models were used (Fig. 8).

In addition to a peak product, cross-correlation values provided us with an additional measure—how much the second waveform had to shift along the first to find the peak cross-correlation value. This value was labelled 'cross-correlation

shift' for our analysis. I performed the same analysis on the shift values of our cross-correlations as were performed on the cross-correlation peak-product. These data were complicated by the fact that decreasing stimulus amplitudes re threshold were associated with unreliable peak locations (Fig. 2). Using only stimulus level re threshold to model, no variation in cross-correlation product be accounted for (R^2 = 7.65e^-0.5). For all tested variables, interactions and higher order modelling did not significantly improve the variation in cross-correlation peak shift accounted for by models.

FFT spectral power analysis

I analysed the spectral variation in neural recordings by conducting a FFT analysis on the ABR waveforms recorded from bat pups. The FFTs of ABRs generally had a similar shape, with maximum spectral amplitudes spanning between 100 and 1000 Hz, a secondary peak in spectral amplitudes occurs between 1000 and 2000 Hz, with multiple diminutive bumps at higher frequencies (Fig. 9). While the FFT data varied, it tended to show a consistent pattern across the DC to 1000 Hz and 1000-2000 Hz ranges, which hereafter will be referred to as the lower and higher spectral ranges, respectively.

To compare the difference between recorded signals labelled as containing an ABR or not containing an ABR, a Welch's t-test was conducted on the average trapezoidal integrals calculated from both frequency bands. For both the lower (T = 16.970, p = 2.15e-62, Cohen's D = 0.37) and higher spectral ranges (T = 8.363, p = 8.46e-17, Cohen's D = 0.18), signals labelled as containing ABRs had significantly more power than those labelled as not

containing an ABR waveform. While amplitudes in both spectral ranges tended to increase over development, the amplitudes in the lower range were consistently higher throughout all age groups and stimulus frequencies compared to the amplitudes in the higher spectral range (Fig. 10). Additionally, the higher spectral range showed significantly larger relative increases in amplitudes over the course of development ($p = 2.17e-13$).

Stimulus level (re threshold) was also effective in accounting for variation in FFT integrals in both the lower ($R^2 = 0.239$) and higher ($R^2 = 0.164$) spectral ranges (Fig. 11). The interaction between stimulus SPL and frequency accounted for a significant sum of the variation in FFT integrals. Calculated FFT integrals for ABRs induced by the tones at the highest stimulus frequencies (80 and 100 kHz) were significantly less sensitive to changes in stimulus level re threshold.

Discussion

Evoked ABRs are a multifeatured signal collected using electrodes placed near but external to the auditory pathway and are thought to represent the summed, far-field response of a collection of more-or-less synchronous neuronal activity (Melcher and Kiang 1996). The ABR is well-known as being an effective and minimally invasive neural recording technique (Burkard et al., 2007). The neural activity reflected in the ABR waveform begins at the cochlear nerve, extending into the brainstem up to higher auditory areas toward the inferior colliculus. Signatures in ABR waveforms have been well documented, showing significant variation with listener attributes (age, head size, hormonal activity, hearing ability) as well as attributes of the sound stimulus (dB SPL, frequency, duration) (Di Lorenzo et al., 1995; Gorga et al., 1987; Don et al., 2005; Stapells & Oates, 1997). While ABRs are a noisy signal, this noise is reduced by averaging many responses to each stimulus; in this thesis, responses were averaged 512 times to produce the resultant ABR waveform.

Using the labels second observer who was blind to the results measured by a more experienced first observer, I have demonstrated that visual labeling of ABR waveform stacks is a reasonably consistent and reliable method for determining evoked thresholds, and that the binary [True/False] and stratified labels [dB re threshold] made by observers relate to the energy and spectral content of the stimulating tone.

Relationships between waveform amplitudes and age, frequency, or stimulating tone sound level were investigated thoroughly using regression. We

found a general trend of increased ABR energy as animals age and/or as stimulus sound level increased. In younger bats, sensitivity to stimulus variables appeared greater than in older bats, where smaller changes to frequency or sound level of the stimulus would cause larger variations in amplitude levels of related ABRs. While this method is effective at finding broad trends between related variables, it can miss nuanced relationships that are not accounted for by the simple models we used. An understanding of expected values of ABR features which this study provides can now allow for more nuanced investigations of relationships between ABR amplitudes and animal or stimulus variables where deviations from expected values can now be modelled.

In this experiment, we chose to present our acoustic stimuli in a free-field sound space as opposed to intra-ear or over-ear stimulation. This introduces some benefits—firstly, the animals will be less irritated by the physical stimulation that the equipment required for over-ear or intra-ear stimuli would produce, potentially leading to animal movement. Secondly, it is easier for the experimenter to replicate physical surroundings between recordings, as the physical interaction between the bat and the equipment is one fewer physical feature to replicate. Finally, it allows for some external validity and understanding of how these tones may affect a bat within their natural environment. A clear disadvantage of free-field stimulation is the lack of control variation in frequency adjustments made by the outer-ear of different bats—if bats have more or less developed pinnae or skulls compared to others of the same-age cohort, then their evoked ABRs will differ no matter how similar the underlying neurology—

thus variations in features of bat ABRs and hearing are influenced both by physical and neurobiological development.

Linnenschmidt & Wiegrebe (2019) were the first to conduct a developmental ABR study in bat pups with the pale spear-nosed bat (*Phyllostomus discolor*) and found a decrease in the RMS amplitude of ABR waveforms with increases in age. In contrast, my study on the development of hearing in *E. fuscus* saw a steady increase in ABR RMS amplitude with pup age (Fig. 12), a result that more closely matches ABR data collected from developing humans (Burkard et al., 2007). This difference could be due to a variety of causes including variability in physical size differences between the animal models tested. The finding of an age-related decrease in the RMS amplitude of ABR recorded from *P. discolor* is interesting because fully grown adult pale speared nosed bats are nearly twice the size of adult big brown bats. Differences in skull width, head shape, and other ABR-related physical features that could arise from morphological differences may explain some of the variation observed between the two bat species. Less apparent physical differences may also account for some differences. For example, in many bat species low frequencies are represented much closer to the ventral surface of the skull compared to higher frequencies, and faint differences in neural arrangement or variations in neural shift over the course of development could also introduce variability in ABR recordings.

We chose to identify ABR thresholds using visual identification and a second observer to verify the results. While slightly conservative, the

observations made by the second observer were extremely similar to the first observer, giving confidence in labels of thresholds. There are at least two reasons why the threshold estimates of the blind observer were more conservative than the original estimates of the 1st observer who collected the data. (1) The 1st observer was more experienced with ABR recording and visual threshold estimation. (2) With the collected data, the blind observer saw more suprathreshold than subthreshold waveforms, hence their threshold estimates were likely to be biased toward higher and more conservative values. The confidence in these labels was essential for feature analysis, given the plan to evaluate the relationship between dB re threshold and many features of concern. We believe that this is the first study to use second observer estimates as a method for establishing confidence in threshold labels for purposes of feature analysis.

On average, the RMS amplitude of ABR waveforms was found to increase over development, although this relationship varied with the frequency of the stimulating tone. In early development, the RMS amplitude of ABR waveforms were relatively equivalent across audible frequencies but would begin to decrease towards ultrasonic frequencies. We know that higher tones have greater energy than lower tones (given equal duration & SPL) suggesting that higher tones may have relatively greater activation than lower tones. However, we also know that lower tones have greater representation along bat basilar membranes. As we did not control stimulus energy relating to either the energy of the stimulus, or the expected representation along the basilar membrane it's

difficult to tease these two features apart in our data. Later in development, when bats acquired hearing sensitivity to higher frequency tones, RMS amplitude-frequency curve (Fig. 13) began to resemble the W-shape of a typical adult *E. fuscus* audiogram (Fig. 2). My analyses also revealed that the amplitude of ABRs evoked in older bats presented with suprathreshold tones started with higher baseline RMS amplitudes whose value increased less within increases in stimulus amplitude re threshold compared to younger bats. This effect may be related to the increased auditory sensitivity associated with aging, where smaller changes in neural energy can accomplish discriminations for older bats that would require a greater difference of energy if presented to pups of a younger age. How the RMS amplitude of ABRs changed with pup age interacted with the frequency of the stimulating tone. As animals aged, the amplitude of ABRs evoked by mid-hearing frequencies (20, 32, and 48 kHz) became relatively more dependent on stimulus amplitude re threshold compared to other tested frequencies where *E. fuscus* is less sensitive (4, 8, 10, 16, 64, 80, and 100 kHz). Given that mid-hearing range overlaps with the same frequencies used in adult *E. fuscus* echolocation and socialization vocalizations, the relative increase in sensitivity at these frequencies could relate to the animal's need for fine spectral and amplitude discriminations of received echoes.

In our bats, ABR feature variability—particularly the timing of waveform peaks and their magnitude—made detecting changes in ABR latency somewhat noisy. Indeed, a peak cross-correlation product shift did not fully capture all the expected changes in response latency to changes in stimulus level . However, as

seen in other animal models, the lag in my calculated correlograms successfully showed that ABRs evoked by lower amplitude pure tones had longer latencies compared to those evoked by higher amplitude counterparts of the same frequency (Fig. 10).

The use of cross-correlation analyses to measure latency changes in evoked ABR waveforms at different sound levels necessitated correlating the ABR signal evoked at the highest SPL signal with each subsequent waveform in a stack collected from the same animal. With the method, no latency was obtained for responses evoked as the highest SPL. A possible workaround could be to use a different technique for this one response and measure the evoked latency visually. Another unforeseen issue associated with the technique I employed was the irregularity with which adjusting stimulus SPLs were reduced when determining hearing thresholds. The irregularity in adjusting stimulus SPL sometimes led to larger gaps between successively collected responses at different sound levels, mainly between 40 to 75 dB SPL. Future studies planning to use multiple cross-correlations to conduct a latency analysis should consider collecting data at smaller and more regular intervals between successively decreasing stimulus amplitude steps as this will provide a higher resolution for assessing latency changes in the evoked response albeit at the expense of longer recording times which could lead to other problems (e.g. increased restlessness and animal movements).

Peak cross-correlation product had a stronger relation than peak cross-correlation shift to both to the detection (i.e., presence/absence) of ABR signals

as well as interactions between animal and different stimulus features. This effect was somewhat expected given the previous RMS amplitude results showing that higher stimulus SPL evoked ABRs with increased energy and therefore were more likely to have a larger peak cross-correlation product. It is important to emphasize that even though ABRs can have a large amplitude in response to higher SPLs, if the evoked waveform does not share similarities to other ABRs within a stack, then a lower cross-correlation product will result. I found a significant sum of variation in the peak cross-correlation product accounted for by stimulus level above threshold (Fig. 7). I found a similar relationship between peak cross-correlation product and stimulus level re threshold, age, and frequency as in the RMS analysis of ABR amplitude for suprathreshold signals—where there was a significant interaction between age, frequency and stimulus level re threshold. As bat pups aged, we found a relative decrease in peak cross-correlation sensitivity to stimuli sound level and an increase in baseline values. This could be representative of the development of facilitative mechanisms along the auditory pathway which enable bats to better hear auditory signals and require less energy differences for discriminations.

In FFTs of the 1-8ms portion of our recorded signals, we found two primary areas of activity. The lower frequency area (0 – 1 kHz) was associated with greater amplitudes, generally being more sensitive to changes in dB re threshold. This lower area was however less sensitive to changes in animal age than the higher frequency area (1 – 2 kHz). Amplitudes in the higher frequency area (1 – 2 kHz) had relatively lower magnitudes than those described in the

lower frequency range (0 – 1 kHz) but this higher range still had a roughly equivalent relationship between energy and stimulus tones, where feature-important tones were greater in magnitude and more sensitive to changes in stimulus level relative to other tones. Many explanations exist which could describe the difference in amplitude patterns between these two areas. It could be that the neural processes which underlay the magnitudes described in the lower frequency areas are more linear in nature relative to the values of their inputs than the processes which underlay the higher frequency section. It is also possible that there is non-auditory activity within the bat's brain relating to either of these two spectral areas, which could lead to increased noise in the measured magnitudes.

In summary, I have described changes in evoked ABR waveforms that reflect transformations in hearing during development in the temperate, insectivorous big brown bat (*E. fuscus)*. The data reveal sizable transformations in auditory sensitivity in bat pups across developmental age groups and in the ability to hear ultrasonic frequencies important for developing the ability to echolocate (Mayberry, Faure, & Ratcliffe 2019; Möckel, et al., 2021). My data also confirm expected changes in ABR waveform features in response to increasing stimulus levels based on a previous developmental study that measured ABRs in the tropical, omnivorous pale spear-nosed bat (*P. discolor*). Using a second observer who was blind to the results measured by a more experienced first observer, I have demonstrated there is reproducibility in visual-labeling of ABR waveform stacks. I have also demonstrated that these labels are

reliable methods for determining evoked thresholds and that binary [True/False] and stratified labels [dB re threshold] as made by the observers relate to the energy and spectral contents of the stimulating tone. The results confirm the W-shaped hearing threshold tuning curve in the big brown bat. I also discuss variations in ABR waveform measures that may relate to increased or decreased auditory sensitivity. The use of ABRs provides researchers with a valuable tool to rapidly collect data from inexperienced and sensitive animals—both for longitudinal studies of hearing across development or the lifespan and/or for field studies where the non-invasive nature of the techniques allows researchers to assess the hearing abilities of bat species in different locations while still permitting the release animals back into the wild.

References

Alpsan, D., & Ozdamar, O. (1992). Auditory brainstem evoked potential classification for threshold detection by neural networks. I. Network design, similarities between human-expert and network classification, feasibility. Automedica, *15*(1), 67–82.

Arnold, S. A. (1985). Objective versus visual detection of the auditory brain stem response. Ear and Hearing, *6*(3), 144–150.

Benichoux, V., Ferber, A., Hunt, S., Hughes, E., & Tollin, D. (2018). Across species “natural ablation” reveals the brainstem source of a noninvasive biomarker of binaural hearing. The Journal of Neuroscience, *38*(40), 8563–8573.

Boku, S., Riquimaroux, H., Simmons, A. M., & Simmons, J. A. (2015). Auditory brainstem response of the Japanese house bat (*Pipistrellus abramus*). The Journal of the Acoustical Society of America, *137*(3), 1063–1068.

Brewton, D., Gutierrez, V., & Razak, K. A. (2018). Accurate sound localization behavior in a gleaning bat, *Antrozous pallidus*. Scientific Reports, *8*:13457. doi.org/10.1038/s41598-018-31606-z

Brittan-Powell, E. F., & Dooling, R. J. (2004). Development of auditory sensitivity in budgerigars (Melopsittacus undulatus). The Journal of the Acoustical Society of America, *115*(6), 3092–3102.

Brown, P. E., Grinnell, A. D., & Harrison, J. B. (1978). The development of hearing in the pallid bat, *Antrozous pallidus.* Journal of Comparative Physiology, *126*(2), 169–182.

Burkard, R. F., Eggermont, J. J., & Don, M. (Eds.). (2007). Auditory evoked potentials: basic principles and clinical application. Lippincott Williams & Wilkins.

Burkard, R.F., & Moss, C. F. (1994). The brain-stem auditory-evoked response in the big brown bat (*Eptesicus fuscus*) to clicks and frequency-modulated sweeps. The Journal of the Acoustical Society of America, *96*(2), 801–810.

Casseday, J. H., & Covey, E. (1992). Frequency tuning properties of neurons in the inferior colliculus of an FM bat. Journal of Comparative Neurology, *319(*1), 34–50.

Cebulla, M., Stürzebecher, E., & Wernecke, K. D. (2000). Objective detection of auditory brainstem potentials: comparison of statistical tests in the time and frequency domains. *Scandinavian audiology*, *29*(1), 44–51.

Charasse, B., Killian, M., Berger-Vachon, C., & Collet, L. (2004). Comparison of two different methods to automatically classify auditory nerve responses recorded with NRT system. Acta Acustica united with Acustica, *90*(3), 512–519.

Chirila, F. V., Rowland, K. C., Thompson, J. M., & Spirou, G. A. (2007). Development of gerbil medial superior olive: integration of temporally

delayed excitation and inhibition at physiological temperature. The Journal of Physiology, *584*(1), 167–190.

Cone-Wesson, B., Dowell, R. C., Tomlin, D., Rance, G., & Ming, W. J. (2002). The auditory steady-state response: comparisons with the auditory brainstem response. Journal of the American Academy of Audiology, *13*(4), 173–187.

Dalland, J., Vernon, J., & Peterson, E. A. (1966). Some electrophysiological aspects of hearing in the bat *Eptesicus fuscus*. *The Journal of the Acoustical Society of America*, *39*(6), 1225–1226.

Delgado, R. E., & Ozdamar, O. (1994). Automated auditory brainstem response interpretation. IEEE Engineering in Medicine and Biology Magazine, *13*(2), 227–237.

Di Lorenzo, L., Foggia, L., Panza, N., Calabrese, M. R., Motta, G., Tranchino, G., Orio, Jr. F., & Lombardi, G. (1995). Auditory brainstem responses in thyroid diseases before and after therapy. Hormone Research in Paediatrics, *43*(5), 200–205.

Don, M., Elberling, C., & Waring, M. (1984). Objective detection of averaged auditory brainstem responses. Scandinavian Audiology, *13*(4), 219–228.

Don, M., Kwong, B., & Tanaka, C. (2005). A diagnostic test for Ménière's disease and cochlear hydrops: impaired high-pass noise masking of auditory brainstem responses. Otology & Neurotology, *26*(4), 711–722.

Ehrlich, D., Casseday, J. H., & Covey, E. (1997). Neural tuning to sound duration in the inferior colliculus of the big brown bat, *Eptesicus fuscus*. Journal of Neurophysiology, *77*(5), 2360–2372.

Elberling, C., & Wahlgreen, O. (1985). Estimation of auditory brainstem response, ABR, by means of Bayesian inference. Scandinavian Audiology, *14*(2), 89–96.

Fenton, M. B. (1984). Echolocation: implications for ecology and evolution of bats. The Quarterly Review of Biology, *59*(1), 33–53.

Fridman, J., John, E. R., Bergelson, M. A., Kaiser, J. B., & Baird, H. W. (1982). Application of digital filtering and automatic peak detection to brain stem auditory evoked potential. Electroencephalography and Clinical Neurophysiology, *53*(4), 405–416.

Froemke, R. C., & Jones, B. J. (2011). Development of auditory cortical synaptic receptive fields. Neuroscience & Biobehavioral Reviews, *35*(10), 2105–2113.

Furuyama, T., Hase, K., Hiryu, S., & Kobayasi, K. I. (2018). Hearing sensitivity evaluated by the auditory brainstem response in *Miniopterus fuliginosus*. The Journal of the Acoustical Society of America, *144*(5), 436–440.

Gabriel, S., Durrant, J. D., Dickter, A. E., & Kephart, J. E. (1980). Computer identification of waves in the auditory brain stem evoked potentials. Electroencephalography and Clinical Neurophysiology, *49*(3-4), 421–423.

Gorga, M. P., Reiland, J. K., Beauchaine, K. A., Worthington, D. W., & Jesteadt, W. (1987). Auditory brainstem responses from graduates of an intensive care nursery: normal patterns of response. Journal of Speech, Language, and Hearing Research, *30*(3), 311–318.

Jen, P. H. S., Zhou, X., & Wu, C. (2001). Temporally patterned sound pulse trains affect intensity and frequency sensitivity of inferior collicular neurons of the big brown bat, *Eptesicus fuscus*. Journal of Comparative Physiology A, *187*(8), 605–616.

Kenyon, T. N., Ladich, F., & Yan, H. Y. (1998). A comparative study of hearing ability in fishes: the auditory brainstem response approach. Journal of Comparative Physiology A, *182*(3), 307–318.

Koay, G., Heffner, H. E., & Heffner, R. S. (1997). Audiogram of the big brown bat (*Eptesicus fuscus*). Hearing Research, *105*(1-2), 202–210.

Kral, A., Tillein, J., Heid, S., Hartmann, R., & Klinke, R. (2004). Postnatal cortical development in congenital auditory deprivation. Cerebral Cortex, *15(*5), 552–562.

Laska, M., Walger, M., Schneider, I., & Von Wedel, H. (1992). Maturation of binaural interaction components in auditory brainstem responses of young guinea pigs with monaural or binaural conductive hearing loss. European Archives of Otorhinolaryngology, *249*(6), 325–328.

Laumen, G., Tollin, D. J., Beutelmann, R., & Klump, G. M. (2016). Aging effects on the binaural interaction component of the auditory brainstem response

in the Mongolian gerbil: effects of interaural time and level differences. Hearing Research, *337*, 46–58.

Linnenschmidt, M., & Wiegrebe, L. (2019). Ontogeny of auditory brainstem responses in the bat, *Phyllostomus discolor*. Hearing Research *373*:85-95.

Macías, S., Mora, E. C., Coro, F., & Kössl, M. (2006). Threshold minima and maxima in the behavioral audiograms of the bats *Artibeus jamaicensis* and *Eptesicus fuscus* are not produced by cochlear mechanics. Hearing Research, *212*(1-2), 245–250.

Mayberry, H. W., & Faure, P. A. (2015). Morphological, olfactory, and vocal development in big brown bats. Biology Open *4*(1):22–34.

Mayberry, H. W., Faure, P. A., & Ratcliffe, J. M. (2019). Sonar strobe groups and buzzes are produced before powered flight is achieved in the juvenile big brown bat, *Eptesicus fuscus*. The Journal of Experimental Biology *222*(20): jeb209163 (doi:10.1242/jeb.209163)

Melcher, J. R., & Kiang, N. Y. S. (1996). Generators of the brainstem auditory evoked potential in cat III: identified cell populations. Hearing Research *93*(1-2):52–71.

Möckel, D., Groulx, T., & Faure, P. A. (2021). Development of hearing in the big brown bat. Journal of Comparative Physiology A, *207*(1):27–42

Møhl, B., & Surlykke, A. (1989). Detection of sonar signals in the presence of pulses of masking noise by the echolocating bat, *Eptesicus fuscus*. Journal of Comparative Physiology A, *165*(1), 119–124.

Moore, D. R. (2002). Auditory development and the role of experience. British Medical Bulletin, *63*(1), 171–181.

Munnerley, G. M., Greville, K. A., Purdy, S. C., & Keith, W. J. (1991). Frequency-specific auditory brainstem responses relationship to behavioural thresholds in cochlear-impaired adults. Audiology, *30*(1), 25–32.

Piczak, K. J. (2015, September). Environmental sound classification with convolutional neural networks. In: 2015 IEEE 25th International Workshop on Machine Learning for Signal Processing (MLSP),1–6.

Pinheiro, A. D., Wu, M., & Jen, P. H. S. (1991). Encoding repetition rate and duration in the inferior colliculus of the big brown bat, *Eptesicus fuscus*. *Journal of Comparative Physiology A*, *169*(1), 69–85.

Shaw, N. A. (1988). The auditory evoked potential in the rat – a review. Progress in Neurobiology *31*(1):19–45.

Simmons, J. A., Moss, C. F., & Ferragamo, M. (1990). Convergence of temporal and spectral information into acoustic images of complex sonar targets perceived by the echolocating bat, *Eptesicus fuscus*. Journal of Comparative Physiology A, *166*(4), 449–470.

Skrinyer, A. J., Faure, P. A., Dannemiller, S., Ball, H. C., Delaney, K. H., & Orman, R. (2017). Care and husbandry of the world's only flying mammals. Laboratory Animal Science Professional June, 24–27.

Song, L., McGee, J., & Walsh, E. J. (2006). Frequency-and level-dependent changes in auditory brainstem responses (ABRs) in developing mice. The Journal of the Acoustical Society of America, *119*(4), 2242–2257.

Song, L., McGee, J., & Walsh, E.J. (2008). Development of cochlear amplification, frequency tuning, and two-tone suppression in the mouse. Journal of Neurophysiology, *99*(1), 344–355.

Stapells, D. R., & Oates, P. (1997). Estimation of the pure-tone audiogram by the auditory brainstem response: a review. Audiology and Neurotology, *2*(5), 257–280.

Trune, D. R., Mitchell, C., & Phillips, D. S. (1988). The relative importance of head size, gender and age on the auditory brainstem response. Hearing Research, *32*(2-3), 165–174.

Virtanen, P., Gommers, R., Oliphant, T. E., Haberland, M., Reddy, T., Cournapeau, D., ... & van Mulbregt, P. (2020). SciPy 1.0: fundamental algorithms for scientific computing in Python. Nature Methods, *17*(3), 261–272.

Walsh, E. J., McGee, J., & Javel, E. (1986). Development of auditory-evoked potentials in the cat. II. Wave latencies. The Journal of the Acoustical Society of America, *79(*3), 725-744.

Wong, P. K., & Bickford, R. G. (1980). Brain stem auditory evoked potentials: the use of noise estimate. Electroencephalography and Clinical Neurophysiology, *50*(1-2), 25–34.

Wrege, K. S., & Starr, A. (1981). Binaural interaction in human auditory brainstem evoked potentials. Archives of Neurology, *38*(9), 572–580.

Zhang, R., McAllister, G., Scotney, B., McClean, S., & Houston, G. (2006). Combining wavelet analysis and Bayesian networks for the classification of auditory brainstem response. IEEE Transactions on Information Technology in Biomedicine, *10*(3), 458–467.

Appendix—Figures

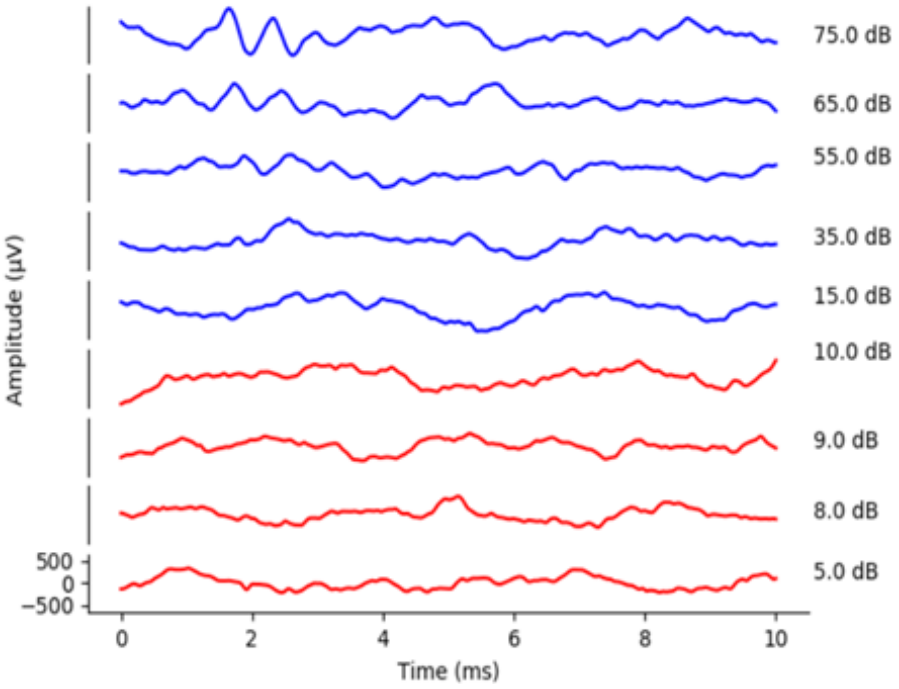

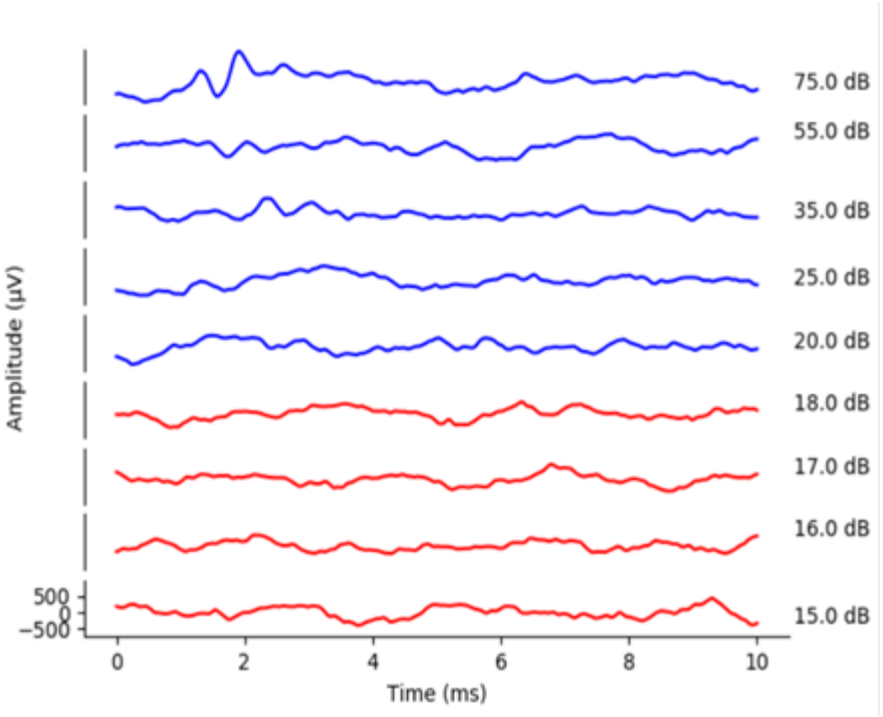

Figure 1. Example averaged ABR waveform ‘stack’, collected at decreasing stimulus amplitudes from a single PND 90 pup at two stimulus frequencies: 20 kHz (*top*) and 48 kHz (*bottom*). Each signal within a ‘stack’ was recorded on the same day. Stimulus onset is at time = 0 ms and had a duration of 5 ms; the ABR recording window was 10 ms. Tones were repeated 512 times at each frequency-level combination. Signals were played with varying dB (usually decreasing) until the lowest amplitude was found which still generated an ABR. Blue traces are signals labelled as above threshold and red traces are signals labelled as below threshold.

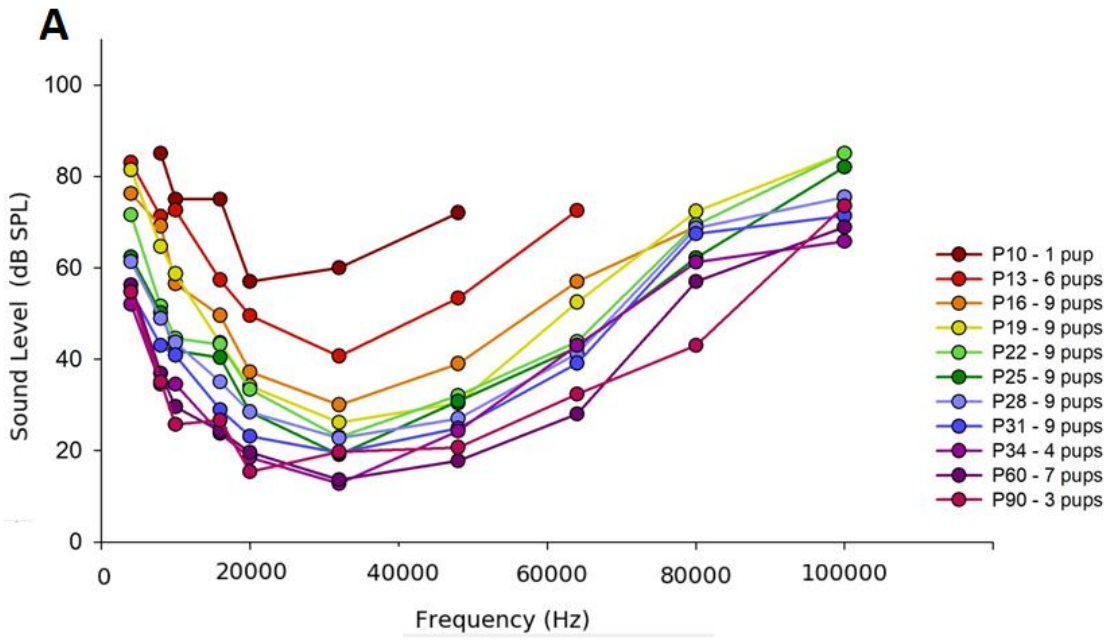
A
Sound Level (dB SPL)
Frequency (Hz)
P10 - 1 pup
P13 - 6 pups
P16 - 9 pups
P19 - 9 pups
P22 - 9 pups
P25 - 9 pups
P28 - 9 pups
P31 - 9 pups
P34 - 4 pups
P60 - 7 pups
P90 - 3 pups

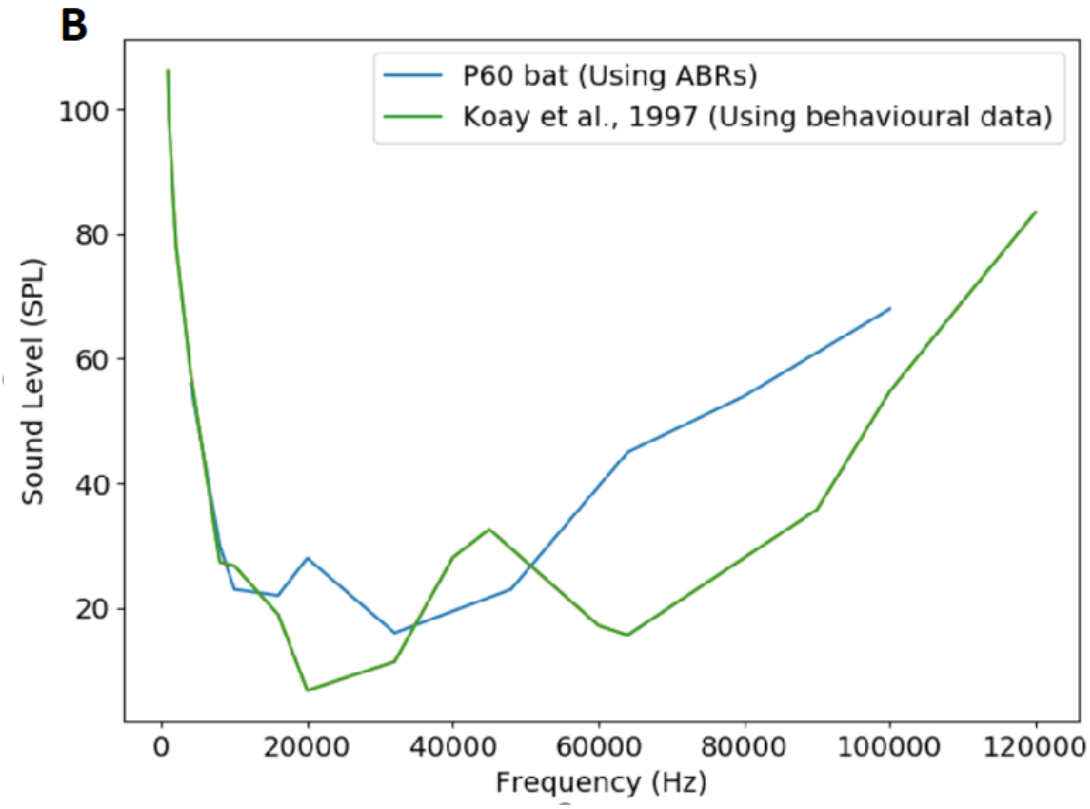
B
P60 bat (Using ABRs)
Koay et al., 1997 (Using behavioural data)
Sound Level (SPL)
Frequency (Hz)

Figure 2. Tuning curves (audiogram) of young adult bats at different post-natal days (PND). A) Average tuning curves for the differently age range in the legend demonstrate a rapid increase in sensitivity over the first 30 days of life, particularly for high frequencies (Möckel et al., 2021). B) A tuning curve for an individual bat at P60 (young adult) from our experiment alongside the previously described W-shaped tuning curve (Koay et al., 1997) gathered with behavioural data from adult bats, with threshold minima at 20 kHz and 60 kHz and a small region of relative insensitivity near 32 kHz between the lowest (4 kHz) and highest (100 kHz) tested frequencies. Audiograms of young adults appear to show a shifted version of the adult audiogram.

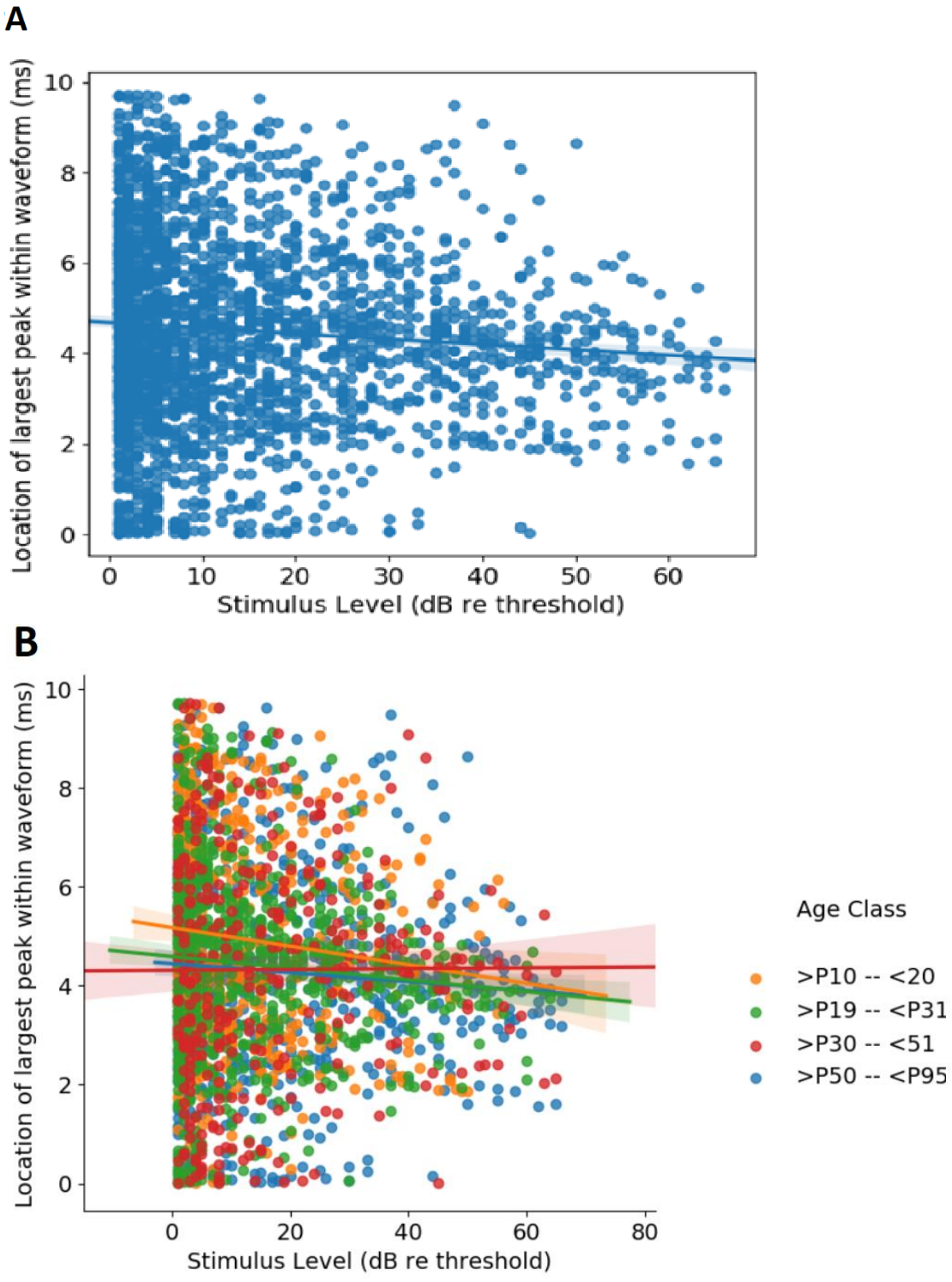
A
Location of largest peak within waveform (ms)
Stimulus Level (dB re threshold)
B
Location of largest peak within waveform (ms)
Stimulus Level (dB re threshold)
Age Class
>P10 -- <20
>P19 -- <P31
>P30 -- <51
>P50 -- <P95

Figure 3. Variation in the temporal position of ABR peaks recorded in developing bat pups. a) The location of the largest peak as a function of level re threshold. Increases in stimulus level relative to threshold appear to decrease average relative latency of the largest peak in ABRs. b) Same information but grouped by age class. Younger pups (lower 2 age classes) appear to have the strongest relationship between latency of highest peak in ABR waveform and stimulus level re threshold. This effect appears to dwindle slightly in young adult bats. The shaded area of each line above represents the 95% confidence interval.

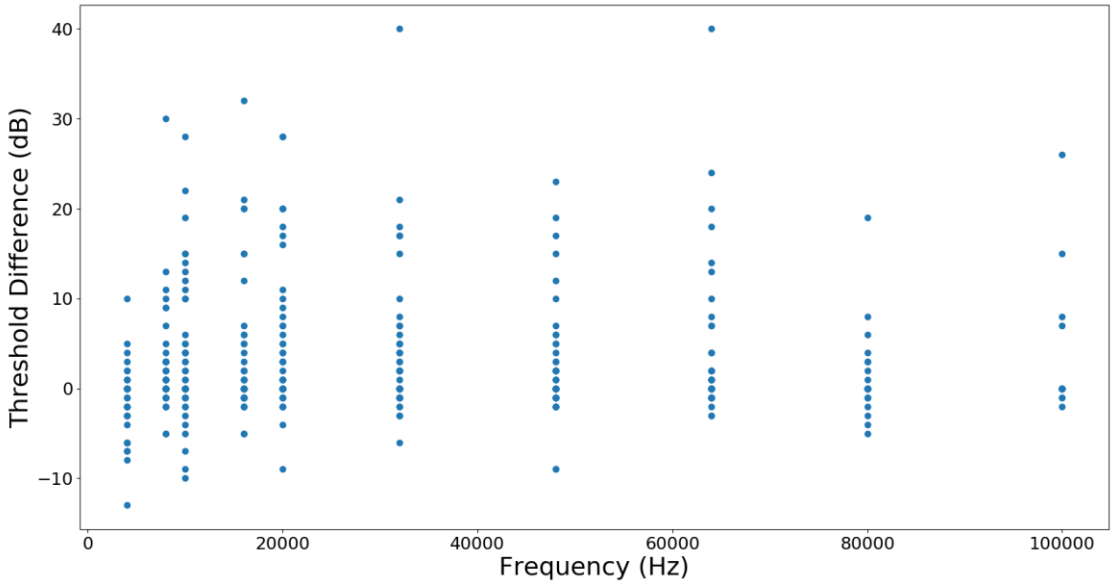

Figure 4. Comparison of independent determination of ABR thresholds as judged by two observers. The first observer measured thresholds online during ABR recordings. A second observer, blind to the threshold estimates of the first observer, re-labelled thresholds from the same data (n = 289 observations from Y pups). Positive values indicate the blind observer judged the ABR threshold to be higher (less sensitive) than the original label during recording. Negative values indicate the blind observer judged the ABR threshold to be lower (more sensitive).

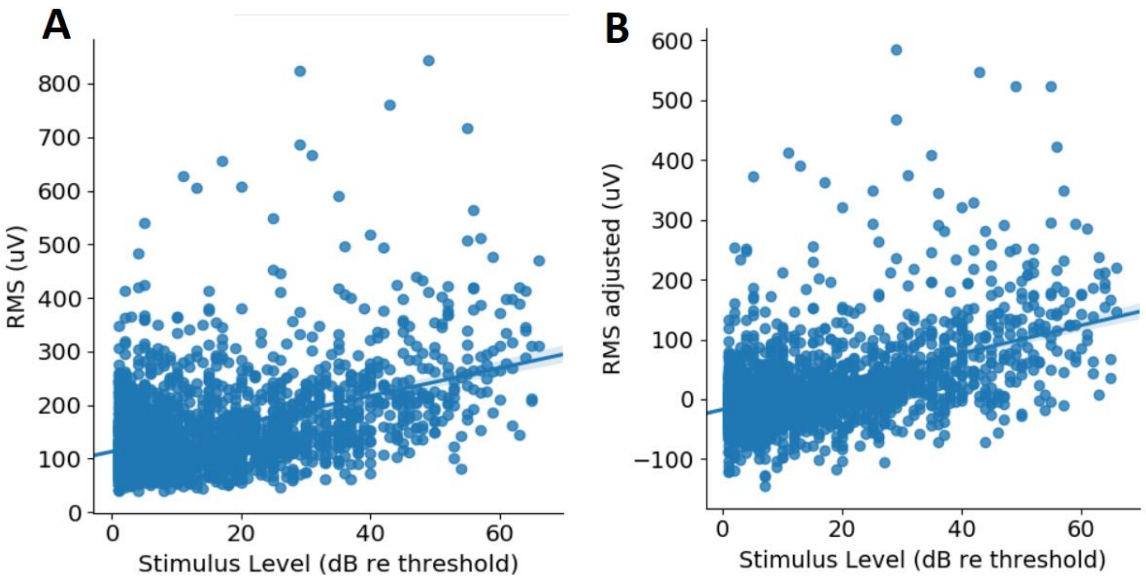

Figure 5. Root mean square (RMS) amplitudes (µV) of recorded ABR signal as a function of stimulus level re threshold, uncorrected for all ages of animal and frequency of stimulating tone. A) Unadjusted regression of RMS shows a general increase in RMS with stimulus level accounting for a significant sum of variance $R^2 = 0.204$; (RMS = dB re threshold * (2.4792) + 116.8637 ± 1.796. B) When the RMS amplitude is adjusted for frequency, day, and animal variance, the relationship improves slightly ($R^2 = 0.253$).

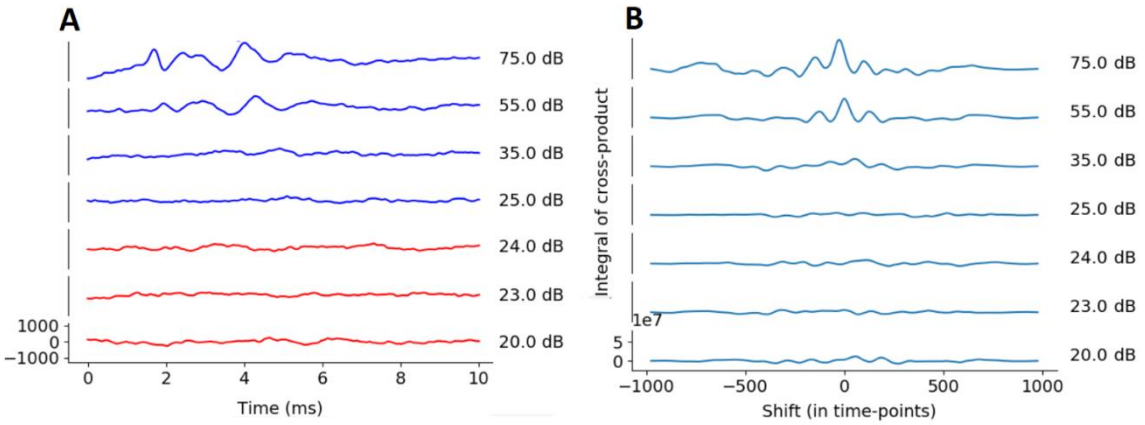

Figure 6. Example ABR waveform stack with its associated cross-correlation function stack. A) Evoked ABRs from a PND 22 bat pup in response to a 32 kHz tone presented at decreasing sound pressure levels (SPLs) from 75 to 20 dB SPL. B) Cross-correlation waveform stack. Each waveform in panel A was cross-correlated with the ABR evoked at the highest SPL to create a cross-correlation stack. In this example, the ABR evoked at 75 dB SPL (*top trace*) was cross-correlated with itself (i.e. auto-correlation) and with each ABR waveform at lower SPLs. As the shape and periodicity of the ABR evoked at 75 dB SPL becomes less related to the shape and periodicity of ABRs evoked at lower SPLs, the height of the central peak within each cross-correlation function becomes smaller and delayed. The *top trace* in the cross-correlation stack is an autocorrelation waveform and its data were not used in later analyses.

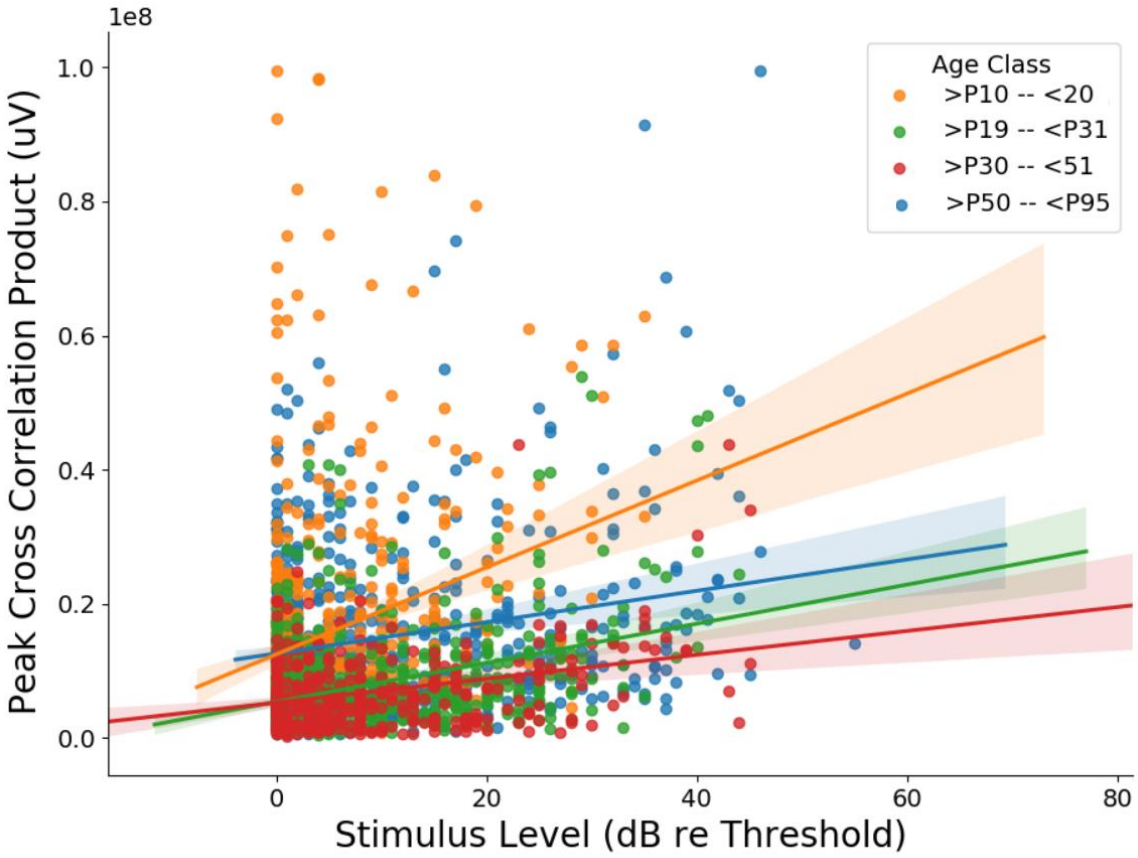

Figure 7. First order linear regression of the peak correlation cross-product value for a given ABRs as a function of the highest stimulus level (re threshold) in its stack. The translucent bands surrounding each regression line represent its 95% confidence interval. As the stimulus level increases above threshold, the peak cross-product of the cross-correlation function also increases. Data are plotted in different colors for different pup age classes. Colored lines are the individual regressions for different age classes. The peak correlation cross-product of younger bats appears to be much more sensitive to changes in stimulus level than those of older bats.

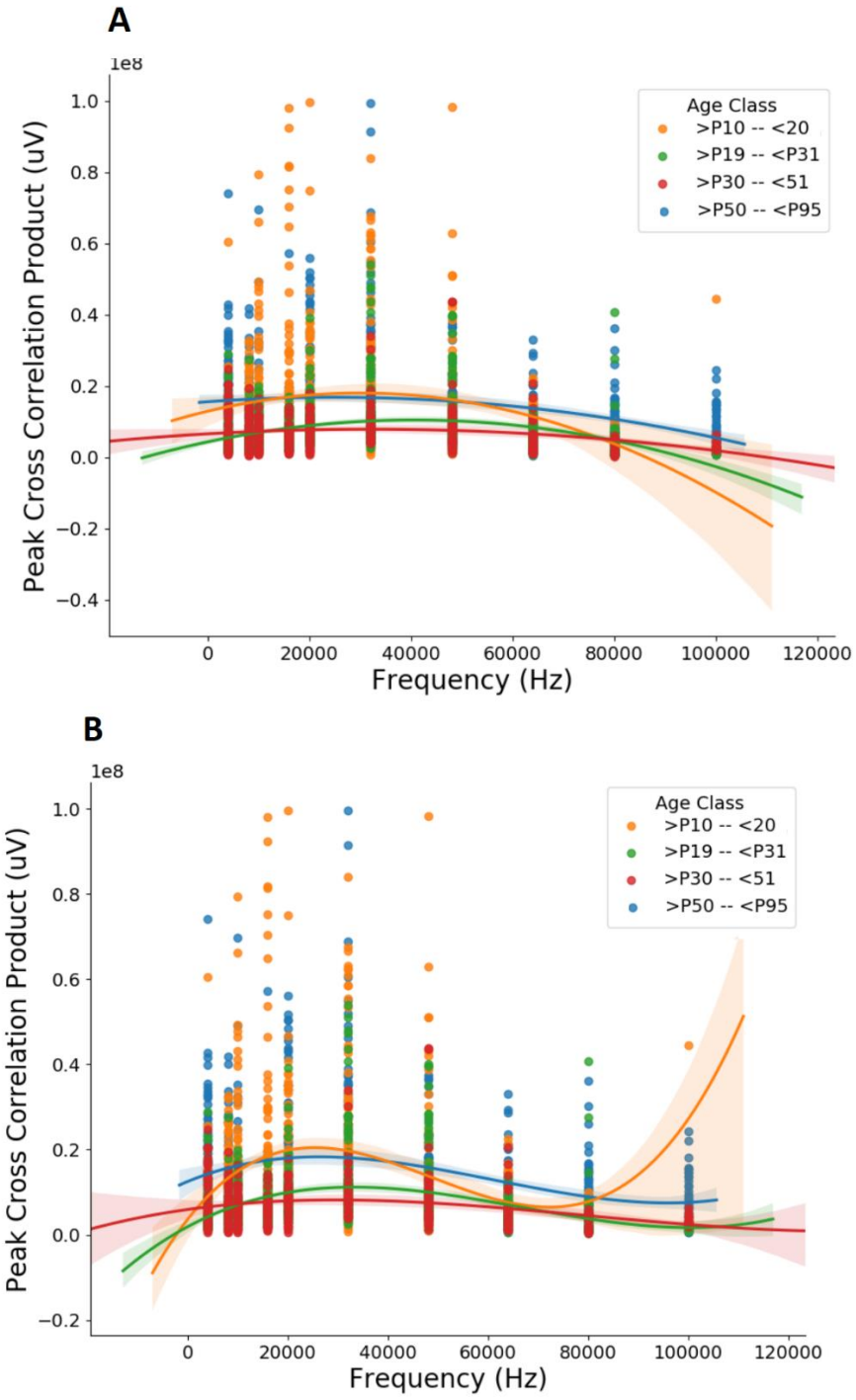
A
1e8
1.0
0.8
0.6
0.4
0.2
0.0
−0.2
−0.4
Peak Cross Correlation Product (uV)
0
20000
40000
60000
80000
100000
120000
Frequency (Hz)
Age Class
>P10 -- <20
>P19 -- <P31
>P30 -- <51
>P50 -- <P95
B
1e8
1.0
0.8
0.6
0.4
0.2
0.0
−0.2
Peak Cross Correlation Product (uV)
0
20000
40000
60000
80000
100000
120000
Frequency (Hz)
Age Class
>P10 -- <20
>P19 -- <P31
>P30 -- <51
>P50 -- <P95

Figure 8. Second (A) and third (B) order regressions of frequency and cross-correlation product. The translucent bands surrounding each regression line represent its 95% confidence interval A) Second order linear model of peak cross-correlation product as a function of stimulus frequency. The mid-range frequencies of hearing for the animal had a slightly stronger relationship with the peak cross-correlation product than lower or higher frequencies. This relationship appeared to shift as bat pups aged and their hearing bandwidth increased, thus increasing their middle hearing range sensitivity. From 20 kHz towards 32 and 48 kHz. B) 3rd As Border model accounted for a greater, but a small sum of variation

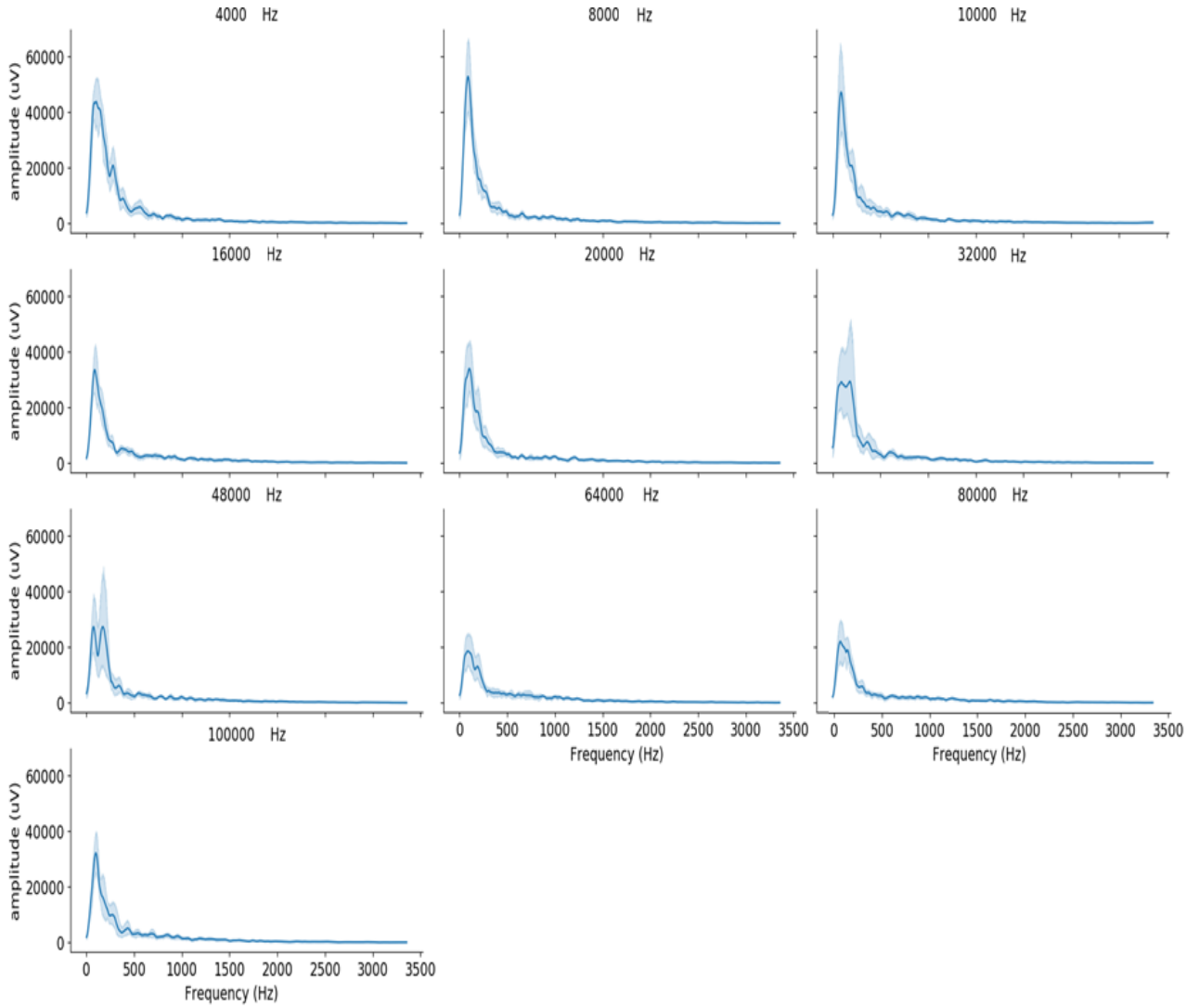

Figure 9. Average fast Fourier transform (FFT) of ABR waveforms evoked from each stimulus frequency. The shaded bands surrounding the waveform represent ±1 SD. Signals used for the FFTs analysis consisted of 976 amplitude measurements that were reduced to 683 amplitude measurements after restricting the analysis to signal amplitudes between 0.1 and 0.8 ms. FFTs used Hanning analysis window (4520 recorded ABRs, 2384 signals recorded as ABRs and 2136 signals recorded and labelled as not containing an ABR).

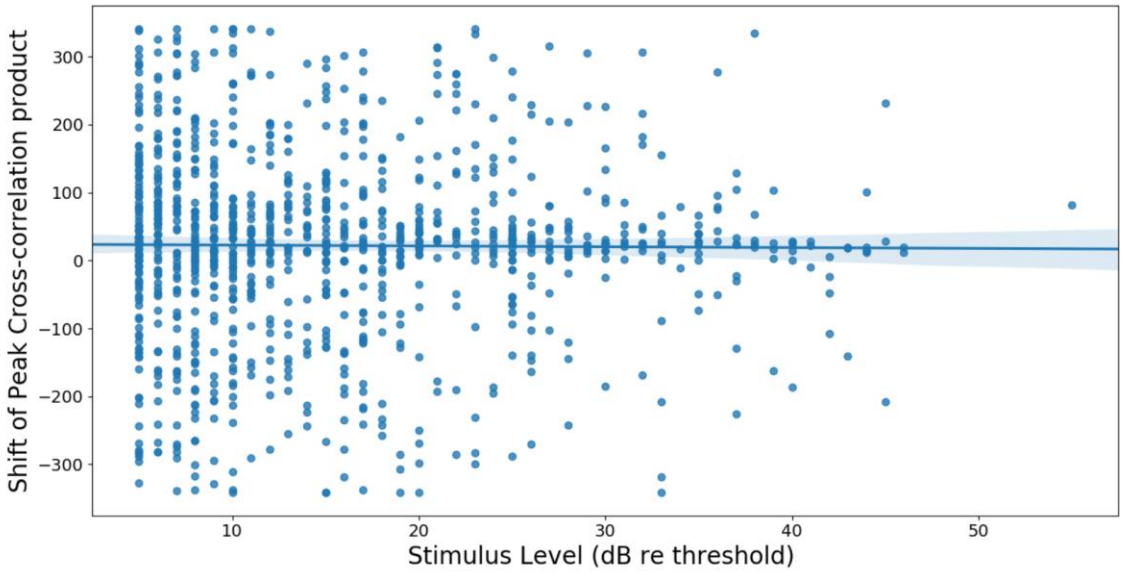

Figure 10. Regression analysis of peak cross-correlation product shift modelled as a function of stimulus level re threshold. The translucent bands surrounding each regression line represent its 95% confidence interval Generally, while having a positive intercept (on average, most signals below the highest SPL tested are positively shifted) there is no effect of stimulus level re threshold on the shift. Largest possible shift of y-axis was +/- 488.

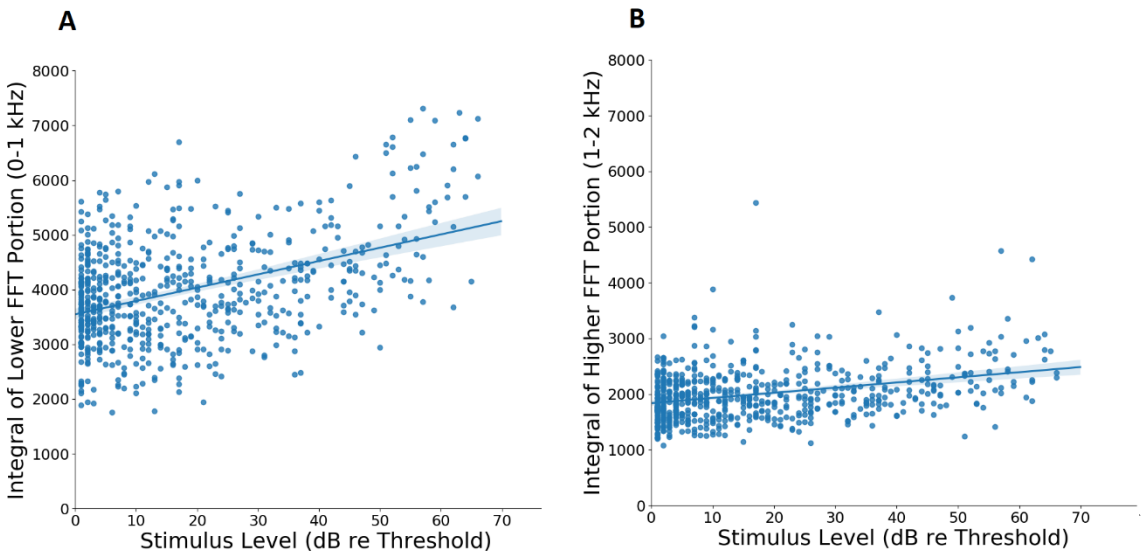

Figure 11. Regression analysis of FFT integrals for two spectral ranges in ABR waveforms. The translucent bands surrounding each regression line represent its 95% confidence interval A) Trapezoidal integral of spectral energy in the range from 0 (DC) to 1000 Hz and B) from 1 to 2 kHz as a function of stimulus level re threshold. In both panels, the integral of the specified zone is positively related to increases in stimulus level re threshold.

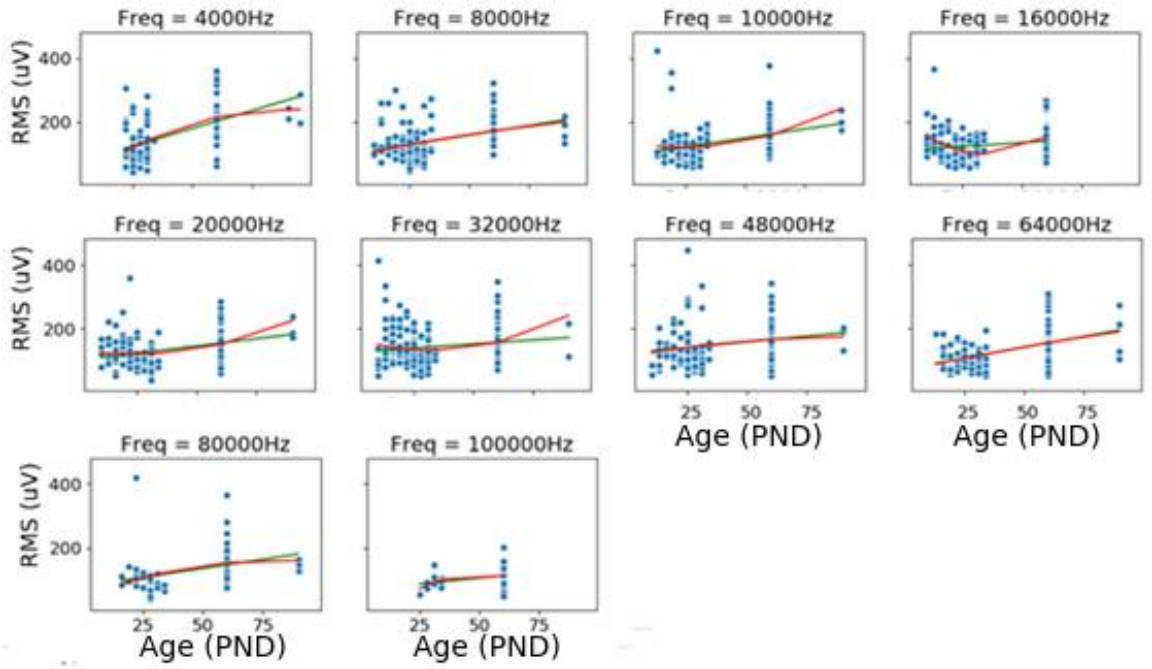

Figure 12. Linear (green) and quadratic (red) regressions of RMS, grouped by frequency, using age as a regressor. For most frequencies (8 kHz, 20 kHz, 48 kHz, 64 kHz, 80 kHz, and 100 kHz), there was little difference between the quadratic and linear regressions. At 16 kHz (R^2 linear = 0.033 and R^2 quadratic = 0.205) there was a significant difference in the variation that quadratic and linear models were able to account for. For some frequencies (20 kHz, 32 kHz, 48 kHz, 64 kHz, 80 kHz, and 100 kHz), the models did not achieve an R^2 above 0.1, while other frequencies showed a better fit (4 kHz: R^2 = 0.289; 8 kHz: R^2 = 0.172;10 kHz: R^2 =0.14). In all cases, there was an increase in the average RMS energy of recorded ABR waveforms with pup age.

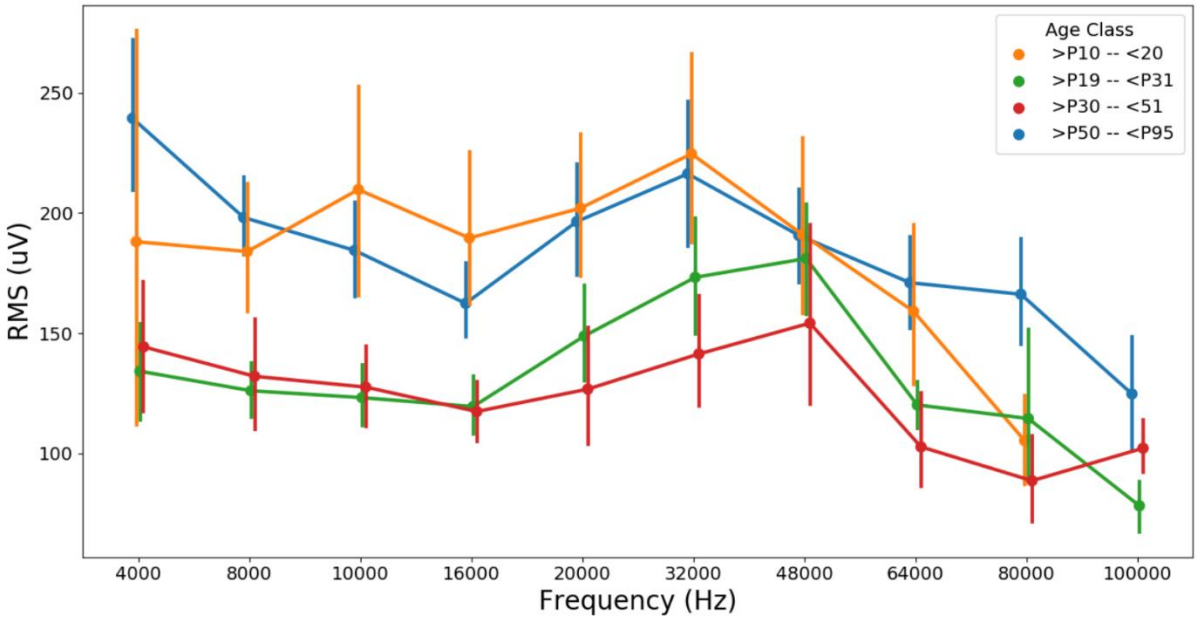

Figure 13. Root mean square (µV) signal amplitude as a function of stimulus frequency (Hz) for increasing age categories in big brown bat pups. Early aging appears to feature relative reductions in RMS amplitude in recorded ABR waveforms while adult-like hearing shows a relative increase. All RMS calculations used a 1 to 8 ms section of the 10 ms ABR recording window.